# Modeling the Impact of African Dust on the Tropical Atlantic Sea Surface Temperature

by

Kelsey Renae Watkins

A thesis submitted in partial fulfillment of the requirements for the degree of

Master of Science
(Atmospheric and Oceanic Sciences)

at the
UNIVERSITY OF WISCONSIN-MADISON
2012

# APPROVED

_____

Dan Vimont, Associate Professor

_____

Date

# ABSTRACT

Climatic changes in the tropical Atlantic over the past few decades are speculated to be due to a number of causes including natural changes, African dust forcing, and anthropogenic causes.  Recent research has shown that the dominant mode of ocean / atmosphere variability in the Atlantic, the Atlantic Meridional Mode (AMM), is excited by variability in African dust outbreaks on interannual to decadal timescales.  These findings conclude that the state of the tropical Atlantic Ocean is directly related to dust emissions over West Africa, which in turn are linked to precipitation and land-use change.  While these findings are suggestive, it is known that a coupled dynamical feedback affects AMM evolution, and hence it is worth exploring the direct and coupled climatic response of the tropical Atlantic to dust forcing in a fully coupled model.

A set of ensemble model experiments was performed using the National Center for Atmospheric Research (NCAR) Community Earth System Model (CESM) to investigate the tropical Atlantic coupled response to African dust emissions.  Each ensemble begins in April and was run for 12 months to capture the seasonality of a boreal summertime dust event.  A heat flux anomaly associated with a typical dust outbreak was used to force the set of model simulations from May through November.  After November, the applied dust forcing is shut off and the coupled

model evolves on its own.  The coupled dynamical response to the imposed forcing is investigated.

The model experiments find that dust forcing can generate a significant response in the tropical Atlantic.  The response to enhanced dust loading includes cooler sea surface temperatures in the northern tropical Atlantic, changes in the surface wind field, and a southward shift in the intertropical convergence zone (ITCZ), especially during the boreal winter following the dust outbreak.  Analysis of the response suggests that the coupled ocean / atmosphere system plays an important role in prolonging the anomalous SST structure, and hence in generating the tropical rainfall anomalies.

# ACKNOWLEGEMENTS

Words cannot express the gratitude I feel toward so many who have helped and supported me in my graduate studies over the last 24 months.  First and foremost, I need to extend an enormous thank-you to Dr. Dan Vimont, my adviser, who has taught me so much in the two years working with him.  He provided a great balance between guidance and independence, allowing me to make mistakes, but more importantly, to make discoveries and breakthroughs.  I feel so fortunate to have had the opportunity to work with him!

In addition, I want to give a huge thank-you to Amato Evan and Ralf Bennartz for their expertise and knowledge.  They have both contributed hugely to my project!  Thank-you again to Ralf Bennartz and also Zhengyu Liu for their wonderful insight on my thesis and for their encouraging words and feedback.

It would be remiss of me not to express my gratitude to the Center for Climatic Research (CCR) especially to Kevin Braun and Julie Niesen.  It has been such an honor to be a part of CCR and Kevin and Julie have both been great in providing me with help and assistance throughout my time on the 11th floor.  Also, a big thank-you goes out to the entire Atmospheric and Oceanic Sciences department, including all staff and faculty, especially Debbie Weber, Angel Skram, Toni Sumner-Beebe, Marrion Ladd, Jan Holmes, and Pete Pokrandt.  All of these individuals have been such a great help!

During my time here at UW-Madison, I have been heavily involved in the DELTA program, which "promotes the development of a future national faculty in the natural and social sciences, engineering, and mathematics that is committed to implementing and advancing effective teaching practices for diverse student audiences as part of their professional careers." I have learned a great deal about teaching and education and have undergone a significant amount of personal and professional growth through my interaction with the students, staff, and professors in the DELTA program.

I need to thank all of the amazing friends in the department I have met and grown to become so close with over the past two years, especially my officemates in Room 1111. The lunchtime chats and outings have been essential to my mental stability regarding research. I could not have made it through graduate school alive without all of them!

Lastly, I would like to thank my family and close friends outside of the AOS department. The support of my friends through Mary Kay, especially to my dear friend Faith, have been amazing in keeping me positive, especially through the rough patches in research. A very special thank-you goes to my parents, my best friend, Brie, and my boyfriend, Matthew. Each of them has provided me with an immense amount of reassurance and encouragement. They have been with me every step of the way on my journey to finishing my master's degree, through the good times and bad. I owe so much of the completion of this degree to them. I can never thank them enough!

# TABLE OF CONTENTS

# List of Figures

# List of Tables

# 1. INTRODUCTION

*a. Background*

Over the last few decades, a topic of interest has been the warming of the tropical North Atlantic sea surface temperatures and a decrease in the amount of African dust emission off of the Sahara desert.  Several scientists have and are investigating the relationship between African dust and its impacts on the ocean, land, and atmosphere.  This study focuses on the impacts of African dust on the tropical north Atlantic sea surface temperatures (SST).  Dust not only has significant weather and climate implications, but also it also affects the micronutrients of phytoplankton in the ocean thus affecting the ocean carbon cycle and atmospheric $CO_2$ (Prospero and Lamb 2003).  Also, during very intense dust outbreaks, the concentration of respirable dust over the Caribbean probably exceeds the U.S. Environmental Protection Agency's 24-hour standard potentially causing health concerns (Prospero and Lamb 2003).

First, it is important to understand the background of African dust impacts. Dust can affect climate in two ways.  It has a direct impact by scattering and absorbing solar radiation and also indirectly through its impact on cloud processes (Prospero 2011).  In Africa, dust blows from the Sahara and Sahel regions westward across the tropical North Atlantic (see Figure 1).  The maximum dust concentrations are typically found between the altitudes of 1.5 km and 4 km, variable between ~1 km and ~5.5 km, a region called the Saharan air layer (Dunion and Velden 2004; Prospero and Carlson 1972). Figures 2 and 3 show the locations of the Sahel and

Saharan regions and also the primary source regions of the dust outbreaks. The dust generation in Africa is determined by soil moisture/rainfall, vegetation coverage, soil properties (both linked to rainfall), wind speed, and land use/disturbance (Prospero 2011). Anthropogenic land use via agriculture, land modification, and land use is difficult to quantify. It was thought the anthropogenic fraction was 30-60% of the total dust loadings, but most recently is estimated to be as little as 10% (Tegen and Fung 1995; Mahowald 2003; Tegen 2004). Figure 4 shows the annual dust emission from natural sources and from anthropogenic-disturbed sources. In addition, over the next century, according to one study, dust loadings are projected to decrease due to land use, carbon dioxide, and human induced climate change (Mahowald and Luo 2003).

Dust emissions across the globe change with the seasons, both in their spatial extent and intensity. Figure 5 is an example of the seasonality of aerosol optical depth. Note the maximum in aerosol optical depth surrounding the Sahara desert and also the seasonal maximum during the boreal summer. The present study focuses on the region just west of the Sahara desert, over the tropical North Atlantic Ocean (see Figure 6). It is easy to see the maximum in dust loading just off the west coast of Africa and the distinct spatial distribution of this dust.

Dust plays a direct role in the sea surface temperature (SST) via increasing or decreasing the radiative heat flux (Foltz and McPhaden 2008a; Foltz and McPhaden 2008b). Atmospheric particles scatter incoming solar radiation and cause regional cooling for areas in which they increase the net backscattering (Schollaert and

Merrill 1998).  In addition, aerosols have been shown to have a large effect on the

coverage and properties of shallow clouds.  In fact, for an increase in the optical

thickness of 0.03 to 0.05, the shallow cloud cover increases by 0.20 to 0.40

(Kaufman et al. 2005).

Figure 7 presents a time series of dust optical thickness in the northern

tropical Atlantic.  A decrease in the amount of dust has been occurring since the

1980s.  Prior to the 1980s, there had been an increasing trend in the amount of dust,

with a maximum in dust in the 1980s. In addition, it has been shown that dust

concentrations are associated with Sahel rainfall (Foltz and McPhaden 2008b).  The

dust maximum in the mid-1980s is related to the drought in the Sahel region in the

early 1980s (Chiapello, Moulin, and Prospero 2005).  A large scale correlation

between Atlantic dust export and Sahel drought during the previous year has been

demonstrated, which suggests that dust emissions in the semi-arid Sahel region are

likely controlled by the placement of the vegetated southern boundary of the Sahara

(Moulin 2004). The oceanic warming around Africa may have weakened the land-

ocean temperature contrast and thus, the monsoon, causing deep convection to

migrate over the ocean and engendering widespread drought over land, from the

Atlantic coast of West Africa to the highlands of Ethiopia (Giannini et al. 2003).  The

warming trend in North Atlantic SST in the recent decades is associated with a

strengthening cyclonic anomaly at 700 hPa in the eastern Atlantic Ocean between

$15^0$-$25^0$N, suggesting a northward shift of the African easterly jet, resulting in

weakening easterlies at latitudes between $10^0$-$20^0$N that reduces dust being blown from Africa into the tropical Atlantic (Wong et al. 2008).

As mentioned, dust has climate impacts and recently, significant changes have been occurring in the tropical North Atlantic.  These changes in the tropical Atlantic Ocean are speculated to be due to natural changes, anthropogenic causes, and African dust forcing.  Ocean temperatures in the eastern tropical Atlantic have been increasing more sharply than have been those in the Caribbean and Western Atlantic, thought to be due to the decreasing dustiness observed over the recent years (Holland and Webster 2007).  Evan and Mukhopadhyay (2010) estimated the amount of radiative forcing by dust from satellite derived aerosol optical depth, for both surface and top of atmosphere (TOA), as shown in Figure 8.  Figure 9 is a time series of surface and TOA forcing by dust from 1955-2008 averaged over the tropical North Atlantic region.  Note a decrease in radiative forcing from the 1950s to 1980s and an increase after the 1980s, a similar trend as seen in the sea surface temperature.  Figure 10 shows the time evolution of North Atlantic SST, and tropical North Atlantic SST over the observed record.  Note that the increase in dust from the 1950s to 1980s (Figure 7) coincides with a decrease in SST over the tropical and entire North Atlantic.  Similarly, from the 1980s to the 2000s, a decrease in dust exists while an increase in SST exists.  Figure 11 displays linear trends of SST, rainfall, and aerosol optical depth (AOD).  Here, SST and AOD are averaged over the tropical North Atlantic region, while rainfall is averaged over the Sahel region.  Foltz

and McPhaden (2008b) claim that the increase in SST is associated with the decrease in AOD due to an increase in rainfall over the Sahel region.

It has even been shown that dust coverage and tropical cyclone activity are strongly inversely correlated over the tropical North Atlantic, but this does not offer solid evidence that the dust itself is directly controlling tropical cyclone activity. It is speculated that a relationship exists between Sahel precipitation and North Atlantic hurricanes (Evan et al. 2006). It was further shown that African dust outbreaks play a non-negligible role in the evolution of eastern Atlantic Ocean temperatures and that the radiative influence of African dust must be considered in predicting changes in tropical cyclone activity (Evan et al. 2008).

To examine the role of dust aerosol forcing on tropical Atlantic SST, Evan et al. (2009) calculate the response of a simple oceanic mixed layer model to surface radiative forcing as derived from a satellite-based estimate of dust aerosol optical depth and a radiative transfer model. They estimated that the mixed layer's response to regional variability in dust aerosol forcing accounts for around 69% of the recent upward trend in northern tropical Atlantic Ocean temperatures. The model output displayed a spatial pattern of the mixed layer response to aerosol surface forcing that looks very similar to the distribution of dust, shown in Figure 12, and also cloud cover and ocean mixed layer depth. Further, they diagnosed this response temporally, as displayed in Figure 13. The right panel shows the observed SSTs over the tropical North Atlantic, while the left shows the mixed layer temperature response to dust and stratospheric aerosol forcing. Figure 14, then,

shows the time series of the observed SST minus the aerosol-forced component from Figure 13.  They estimated that about 67% of the detrended low frequency variability in northern tropical Atlantic temperatures is driven by local variations in aerosol loadings.  Their study, however, does not include analysis of coupled and dynamical feedbacks to aerosol forcing of tropical ocean temperatures. (Evan et al. 2009)

Evan et al. (2011) performed simulations with an ocean general circulation model forced with a record of surface radiation from anomalous dust concentrations in the atmosphere.  The dust record, reconstructed from a coral proxy and satellite retrievals, is shown in Figure 15.  The map in Figure 15 shows the spatial structure of the Atlantic Meridional Mode (AMM) and the structure of the sensitivity of SST to dust variability.  The similarity between the structure of the AMM and ΔSST indicates the projection of dust forcing onto the AMM.  Further, they diagnosed the AMM time series into observed and dust-forced components.  In Figure 16, the observed AMM time series and the dust-forced component of the AMM are compared, and show strong similarity between the observed and dust-forced AMM indices generated by direct forcing of the AMM by African dust outbreaks.  (Evan et al. 2011)

Lastly, the response of dust forcing was investigated in an idealized coupled model and output is shown in Figure 17.  The idealized dust forcing, shown in Figure17a, was applied over months 1-4, after which the forcing is shut off and the idealized model evolves on its own.  Figure17b-i show the response in monthly

mean SST, boundary layer pressure, and boundary layer winds for model months 1-8.  A clear equatorward and westward evolution of the model response exists and is strong in the equatorial region.  This indicates that there may be a coupled equatorial response to Atlantic dust outbreaks in nature.  (Evan et al. 2011)

*b. Motivation*

The findings of Evan et al. (2011) motivate further examination of how dust aerosol radiative forcing can influence tropical Atlantic SSTs.  In particular, the bulk of Evan et al. (2011) investigates the response of an uncoupled ocean model to dust aerosol radiative forcing.  Furthermore, coupled effects are inferred using a very simple coupled model with very simple parameterizations of surface fluxes and of the atmospheric response to SST anomalies.  The primary question is how will a more realistic model respond to realistic dust forcing?  A long record model simulation and a series of ensemble sets were performed to investigate this dust response.  A fully coupled model experiment is a useful extension of the work that has already been done, allowing examination of coupled feedbacks and more realistic coupled processes.

This manuscript is organized as follows: the model itself as well as the model setup and the method of dust forcing will be explained in Section 2.  Section 3a will show the results from the primary experiment, with Section 3b explaining the mechanism behind the response.  Section 3c will present the results from sensitivity

studies.  Finally, Section 4 will discuss the conclusions, implications, caveats, and

future work of this study.
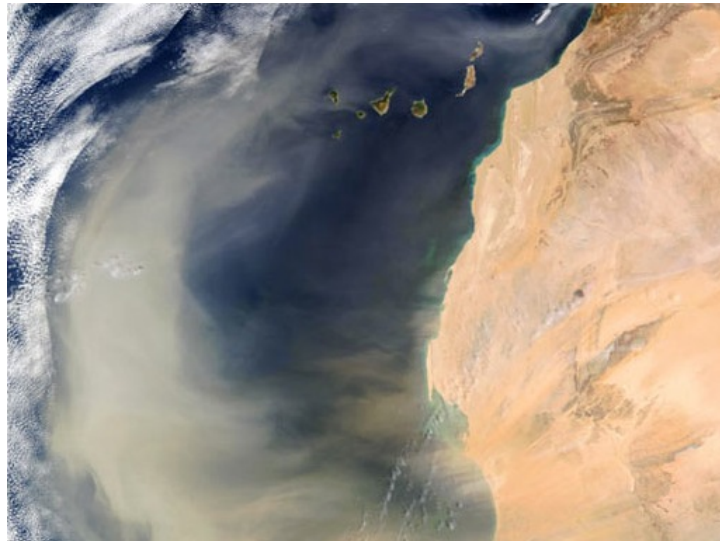
Figure 1. (Taken from MODIS Aqua; NASA 2008) Satellite image of a dust outbreak off the coast of the western Sahara desert in Africa.
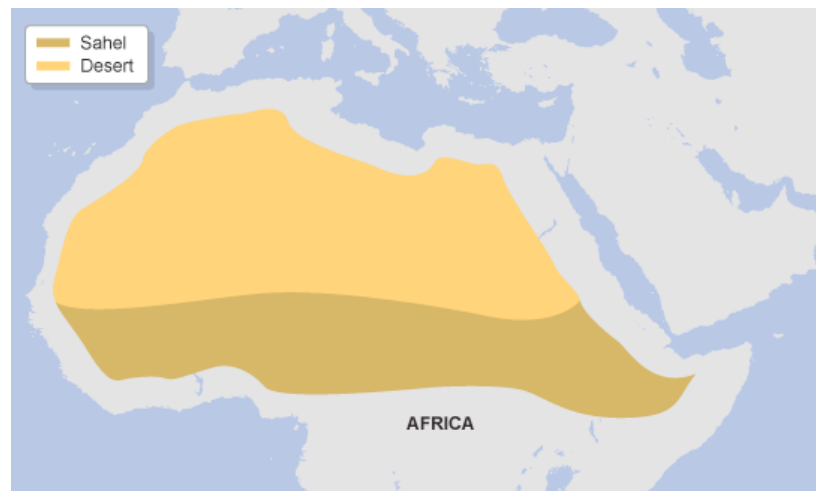


Figure 2. (Taken from BBC 2012) Map of the Sahel and Saharan desert regions.
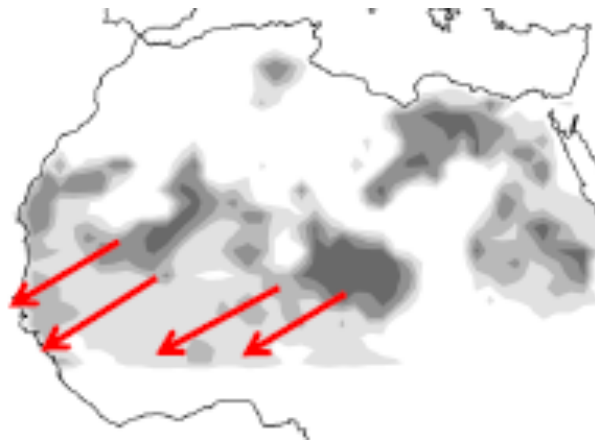
Figure 3. (Taken from Figure 4 of Prospero et al. 2002) Map of TOMS dust source regions across the Sahara desert of northern Africa.
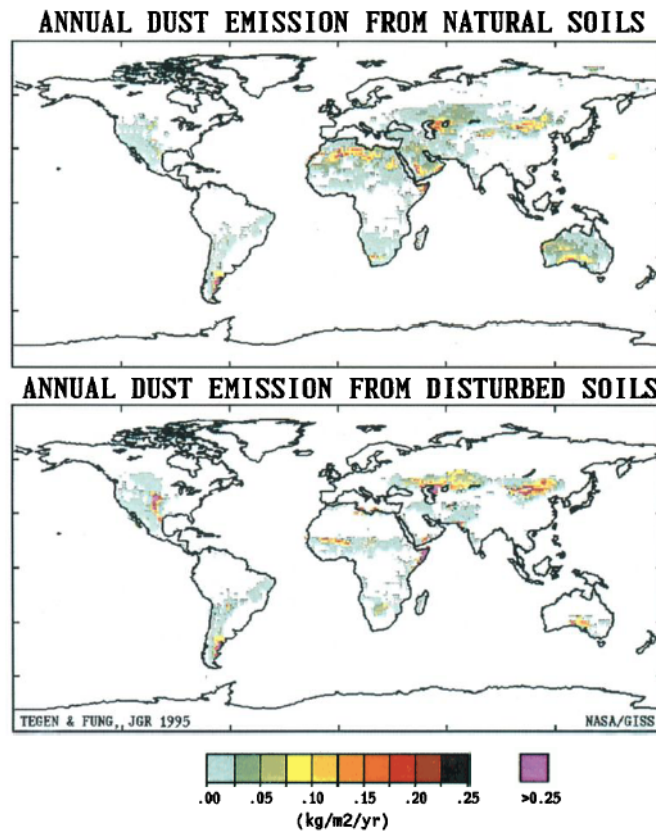


Figure 4. (Taken from Plate 2 of Tegen and Fung 1995) Distribution of modeled annual dust emissions from natural sources (top) and anthropogenic disturbed sources (bottom).
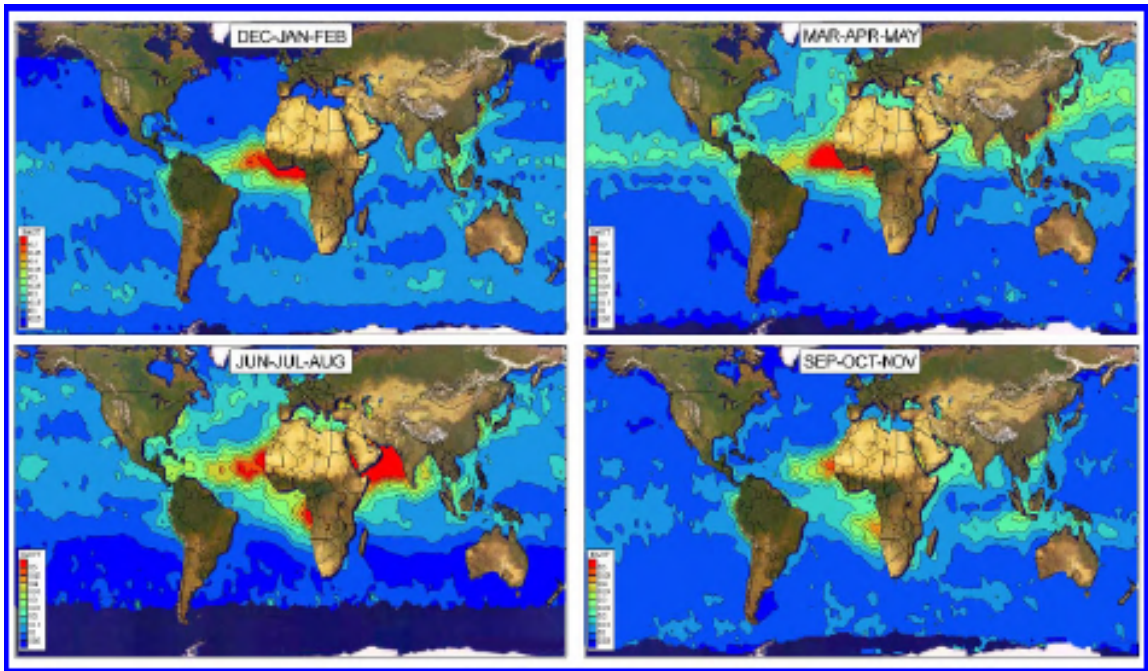
Figure 5. (Taken from Plate 1 of Husar, Prospero, and Stowe 1997) Radiatively equivalent global aerosol optical depth for July 1989 to June 1991 derived from National Oceanic and Atmospheric Administration (NOAA) Advanced Very High Resolution Radiometer (AVHRR) satellites.
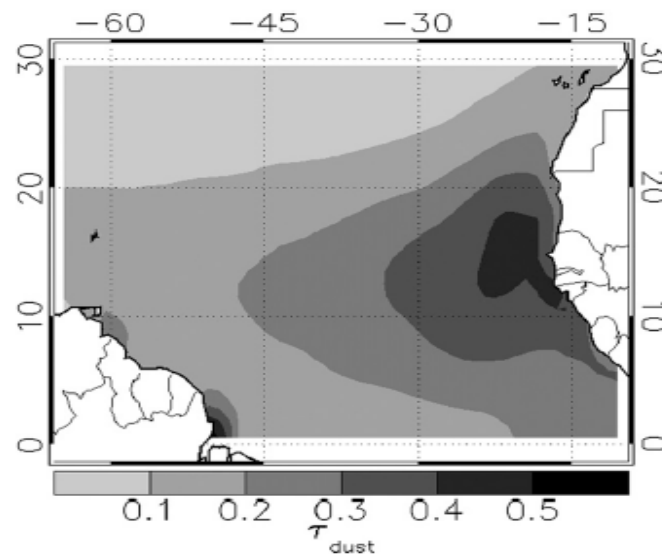


Figure 6. (Taken from Figure 12 of Evan and Mukhopadhyay 2010) Map of the long-term mean dust optical thickness for the period 1955-2008, based on output from a statistical model that extends satellite estimates of dust optical thickness back in time.
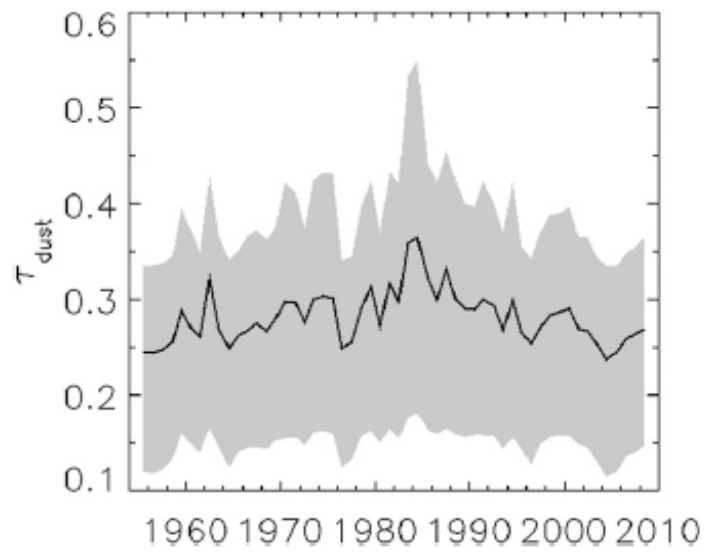
Figure 7. (Taken from Figure 13 of Evan and Mukhopadhyay 2010) Time series of mean northern tropical Atlantic reconstructed dust optical thickness. Gray region represents the range of monthly-mean values for each year; thick black line is annual-mean. Values averaged over the area 5-20ºN and east of 50ºW.
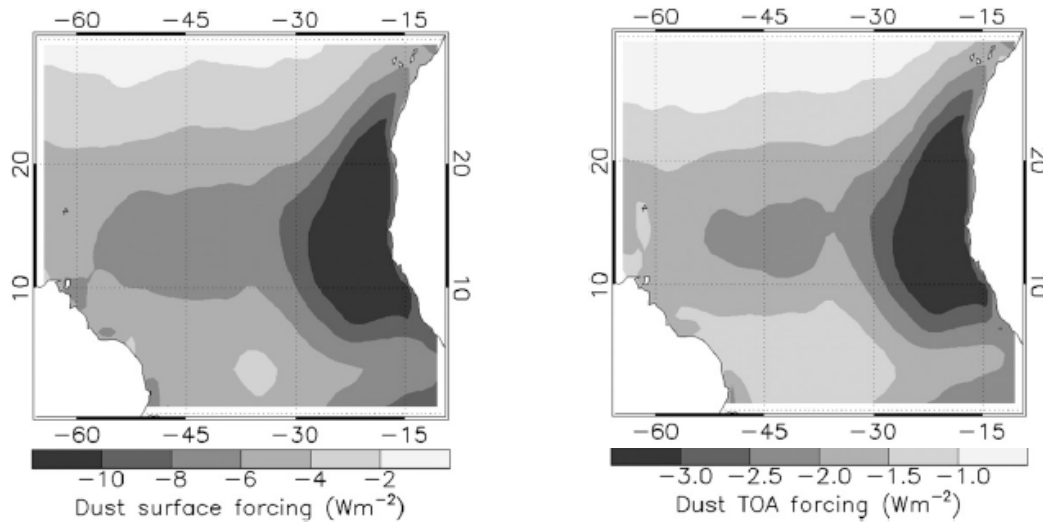
Figure 8. (Taken from Figure 18 of Evan and Mukhopadhyay 2010) Long-term mean (1955-2008) all-sky climatological average of surface downward radiative forcing by dust (left) and top of atmosphere (TOA) radiative forcing by dust (right).
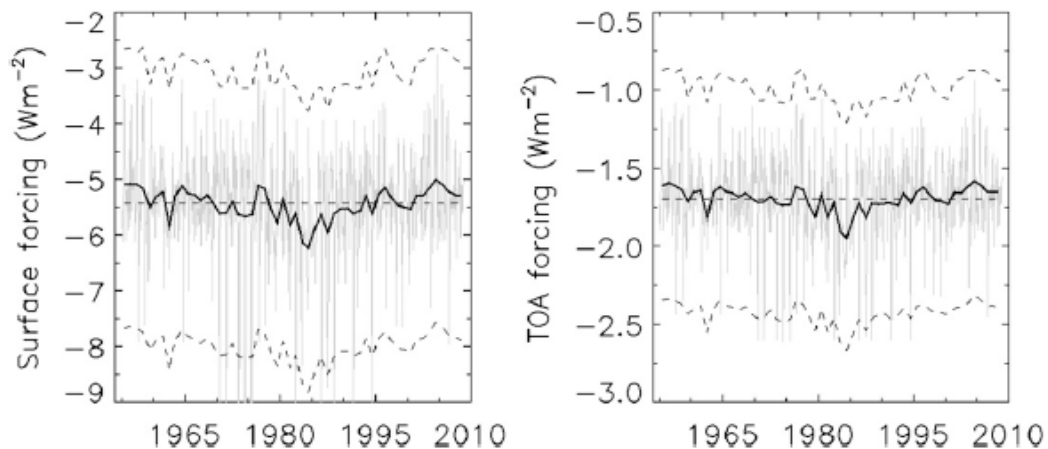


Figure 9. (Taken from Figure 20 of Evan and Mukhopadhyay 2010) Time series of surface (left) and TOA (right) forcing by dust. Monthly (gray line) and annual mean (black line) time series of dust surface forcing are for the period 1955-2008 and averaged over the region of 5-20ºN and east of 50ºW. Monthly mean values are shown without the seasonal cycle. The dashed lines indicate uncertainties in the annual mean time series associated with errors in dust optical thickness.
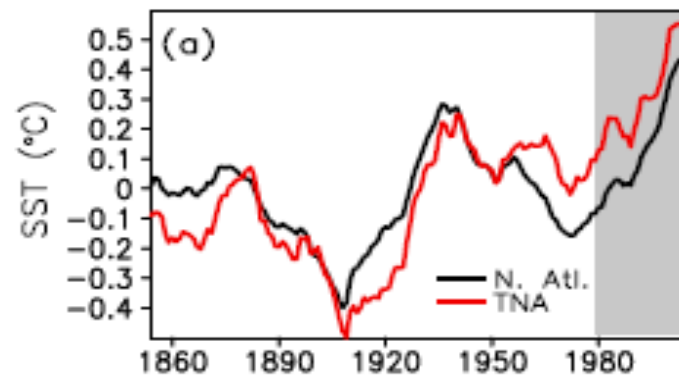
Figure 10. (Taken from Figure 1 of Foltz and McPhaden 2008b) North Atlantic (0-60ºN, 15-75ºW; black line) and tropical North Atlantic (5-25ºN, 10-60ºW; red line) sea surface temperature indices during 1854-2006**.**
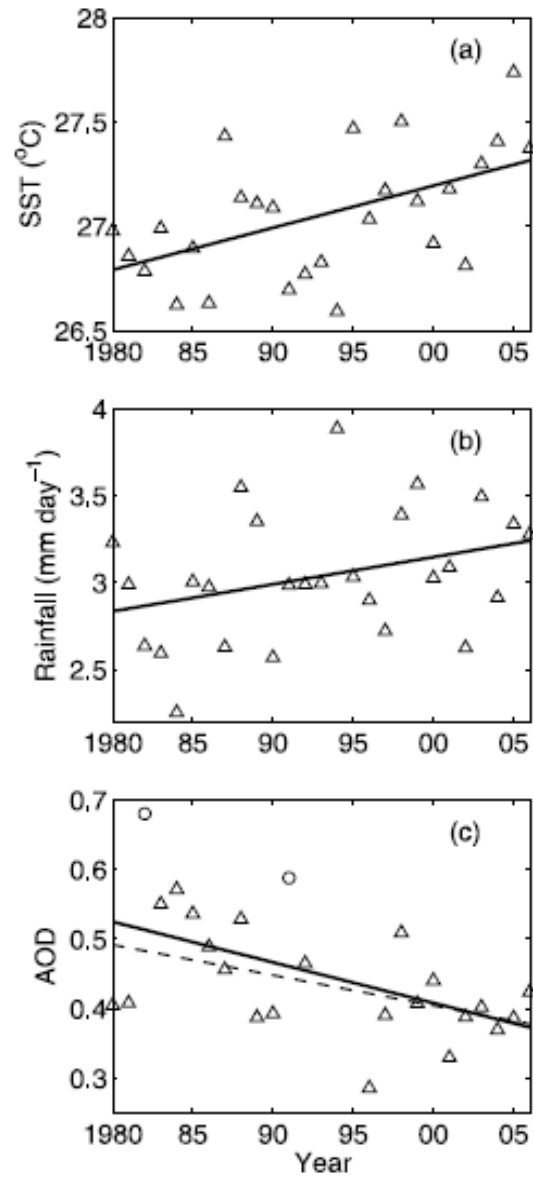
Figure 11. (Taken from Figure 2 of Foltz and McPhaden 2008b) June-September means (triangles) and linear trends (sold lines) in (a) tropical North Atlantic SST, (b) Sahel region rainfall, and (c) tropical North Atlantic aerosol optical depth. Circles in (c) denote the years of significant volcanic eruptions (1982 and 1991). Dashed line is the linear trend calculated after removing these data points.
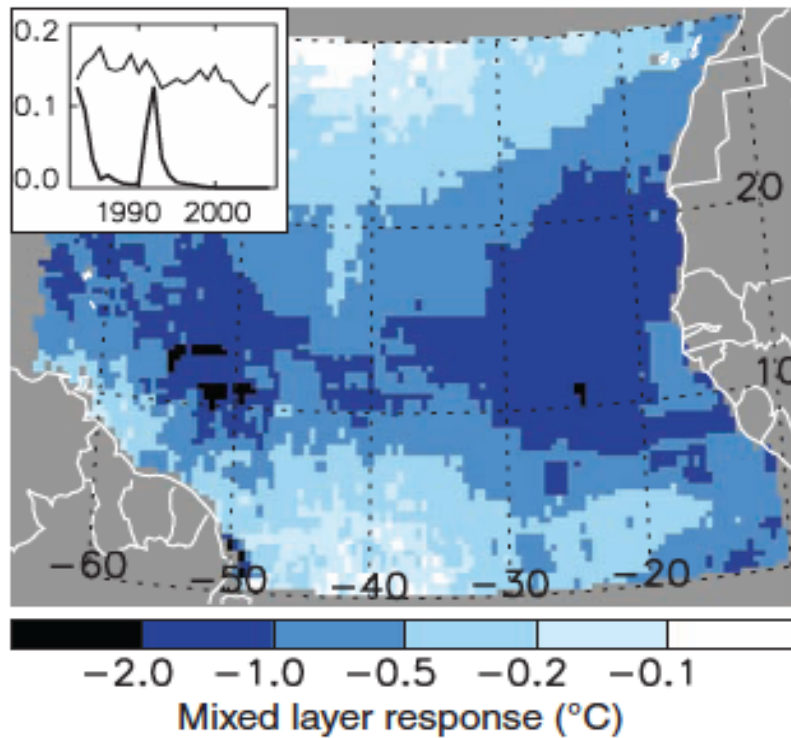
Figure 12. (Taken from Figure 1 of Evan et al. 2009) Map of the mixed layer response to the presence of dust and volcanic aerosols and time series of aerosol optical depth. Estimations of mixed layer temperature response to surface radiative forcing by mineral dust and stratospheric volcanic aerosols are averaged over the 1982-2007 period and have a spatial resolution of 0.5 degrees. The inset plot is a time series of annual mean monthly dust optical depth (thin line) and stratospheric aerosol optical depth (thick line), both averaged over the tropical Atlantic (0-30ºN, 15-65ºW).
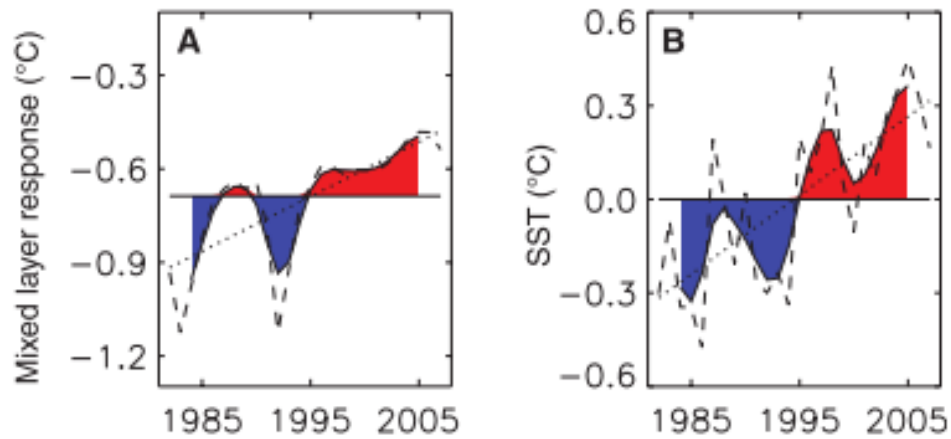
Figure 13. (Taken from Figure 2 of Evan et al. 2009) Time series of mixed layer response to dust and stratospheric aerosol forcing (A) and observed SST anomalies (B).  Both are averaged over the tropical North Atlantic (0-30°N, 15-65°W) and the dashed line is the annual mean, the thin solid line is the climatological mean, the dotted line is the linear least-squares trend, and the thick black line is the annual mean time series with a 1-4-6-4-1 filter.  Red and blue regions correspond to periods that are above and below the climatological mean, respectively.
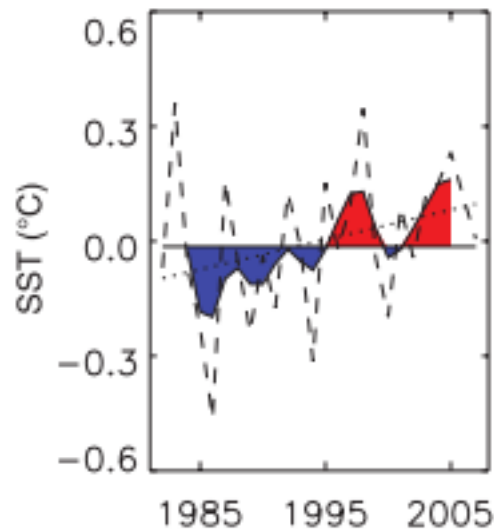


Figure 14. (Taken from Figure 3 of Evan et al. 2009)Anomaly time series of observed SST minus the aerosol forced component from previous figure.  Description is otherwise the same as for Figure 13.
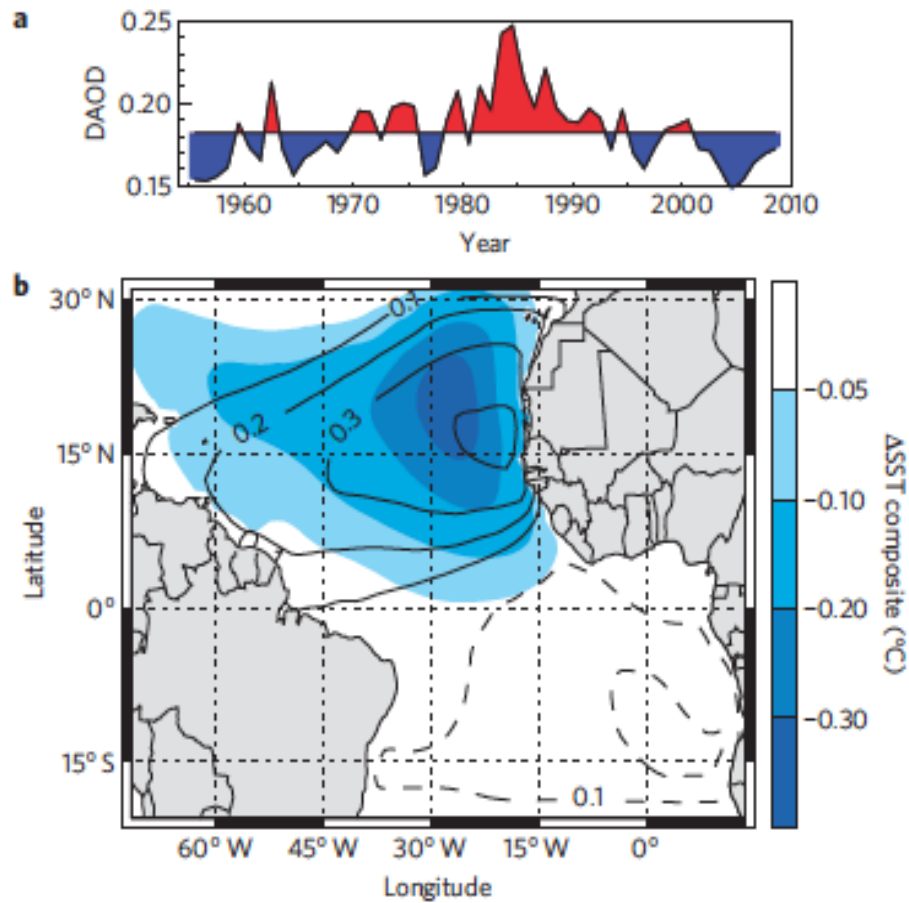
Figure 15. (Taken from Figure 1 Evan et al. 2011) The annual time series of dust aerosol optical depth (DAOD) averaged over the region 10-20ºN and 20-50ºW (a). Contours of the spatial structure of the AMM with composite differences of the ΔSST for the 5 years of highest and lowest DAOD shaded, representing the structure of the sensitivity of SST to dust variability.
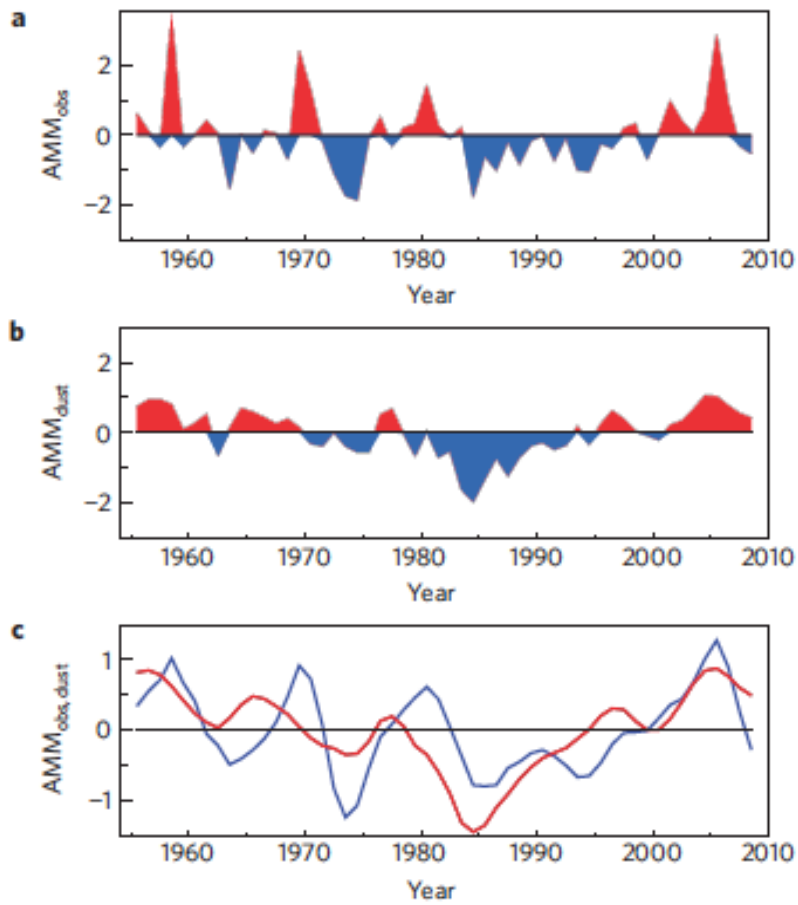
Figure 16. (Taken from Figure 3 Evan et al. 2011) The annually averaged observed AMM time series (a), the dust-forced component of the AMM (b) and the 5-year low-pass-filtered observed (blue) and dust-forced component (red) of the AMM (c).
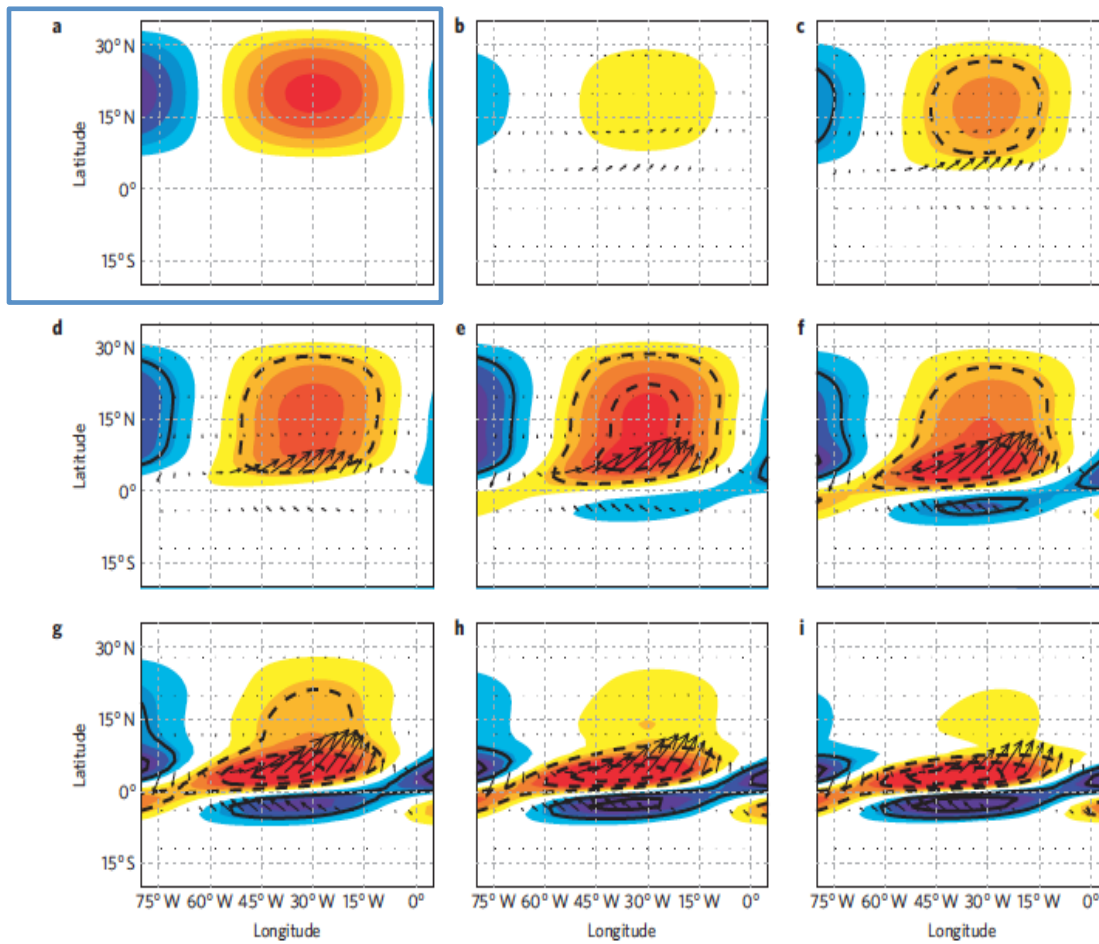
Figure 17. (Taken from Figure 2 Evan et al. 2011) The idealized dust forcing (K d$^{-1}$) used to force a coupled model during the first four months. (a) The equatorward and westward evolution of the model response in monthly mean SST (shaded), boundary layer pressure (contours), and boundary layer winds (vectors) for model months 1-8. (b-i) Positive (negative) SST anomalies are shaded red (blue) and positive (negative) pressure anomalies have solid (dashed) contours, and the zero line has been omitted. Units are arbitrary but consistent throughout b-i.

## 2. METHODS

*a. Community Earth System Model (CESM)*

The Community Earth System Model (CESM) is developed at the National Center for Atmospheric Research (NCAR) and primarily supported by the National Science Foundation (NSF). It is a state-of-the-art fully coupled, global climate model for simulating the Earth's past, present, and future climate states. Five separate models, including atmosphere (atm), ocean (ocn), land (lnd), land-ice (glc), and sea-ice (ice), all work simultaneously through a central coupler component (cpl). (See Figure 18.) The CESM system can be configured a number of different ways and it supports several different resolutions and component configurations. In addition, each model component has input options to configure specific model physics and parameterizations. (Vertenstein et al. 2012)

The component set configuration used in this study is the E_2000 component set. This component set represents present day conditions, with fully active dynamical atmosphere, land, and sea-ice components, meaning they are fully prognostic. The E_2000 component set has a slab ocean model that computes updated SSTs based on prescribed ocean heat flux convergence, mixed layer depths, atmosphere/ocean, and ice/ocean fluxes that are obtained from the coupler (described below). Lastly, this component set has no land-ice model. The atmosphere and land models have a finite volume grid at approximately 2 degrees resolution, whereas the ocean and ice models have a displaced pole grid at approximately 1 degree resolution. (Vertenstein et al. 2012)

Because this configuration utilizes a fully active atmosphere model with a slab ocean model, it is important to understand both the atmosphere component and slab ocean model.  The atmosphere model in this case is the Community Atmosphere Model, version 4 (CAM4) that has 26 vertical levels and contains non-interactive aerosols.  The slab ocean model includes prescribed ocean heat transport, or Q-fluxes, that are obtained from a preexisting fully coupled simulation.  The following equation is used to calculate the heat content of the oceanic mixed layer, from with SST is obtained:

$$\rho c_p h_{mix} \frac{dT_{mix}}{dt} = F_{net} - Q_{flx} \qquad (1)$$

where $h_{mix}$ is the depth of the mixed-layer; $T_{mix}$ is the mixed-layer temperature; $F_{net}$ is the net surface heat flux including the atmosphere-to-ocean and ocean-to-ice surface and basal fluxes, sensible (if any) and latent heat from snow falling into the ocean, sea ice growing over open ocean, and "runoff"; and $Q_{flx}$ is the implied horizontal and vertical flux of heat into/out of the local mixed-layer column by oceanic processes.  The mixed-layer depths are allowed to vary geographically and are fixed (i.e. not time varying).  The assumption is that the ocean temperature is well-mixed and that the SST is the same as $T_{mix}$. (Bailey et al. 2010; Bitz et al. 2011)

*b. Model Setup*

Within the CESM framework, many options exist.  As mentioned, the component set used here is the E_2000 component set, which is a present day

simulation that couples a fully-active atmosphere model, land model, and sea-ice model with a slab ocean model. After creating a case for a new model run, three options exist for how the new CESM run will be initialized, including 'startup', 'hybrid', or 'branch.' For a startup run, initialization occurs independently by each component and can include the use of restart files, initial files, external observed data files, or internal initialization. In this case, the coupler does not need an input data file because it is initialized internally by the model component set. In a branch run, each component is initialized using a consistent set of restart files of a previous model run. The start date for the branch run is defined by the restart date from the existing run. The new case is able to produce an exact bit-for-bit restart in the same manner as the existing run if no modifications are made. (Vertenstein et al. 2012).

This study investigates the role of dust forcing in generating tropical Atlantic variability. As such, we compare two sets of model simulations: a control simulation with climatological dust forcing, and a set of ensemble simulations in which dust aerosol radiative forcing associated with a "typical" dust outbreak is applied at the ocean surface. The startup run was used for the control simulation, which ran continuous for 50 years (Table 1). We discard the first 10 years of the control simulation to allow for model spin up. Three ensembles of branch simulations were used to investigate the response due to dust and to perform sensitivity experiments. Each of the branch simulations (green lines in Figure 19) was initialized on April 1 from the existing control simulation (red line in Figure 19) and was integrated forward for 12 months. Dust aerosol forcing (described below)

is applied to each member of the branch simulation from May through November, and then shut off, allowing the model to run in an unforced coupled mode from December through the following March. Note that the model interpolates boundary conditions from mid-month values, so forcing linearly ramps up from April 15 through May 15 and linearly ramps down from November 15 through December 15.

The primary set of ensembles (e2000branch) contained 40 branch simulations (i.e. ensemble members), each with dust forcing as described above. The branch runs were initialized every April 1st from years 10 through 49 from the control. Two other sets of ensembles of 20 members each were performed with half-amplitude forcing (e2000branch.half) and with the polarity of the forcing reversed (e2000branch.neg). These sets were also initialized every April 1st, but only from years 10 through 29 from the control.

*c. Dust Forcing*

Each ensemble branch simulation was forced with some type of dust forcing. The primary set of ensembles is designed to represent a boreal summer with relatively intense dust activity. Boreal summer was chosen as this season experiences large dust loadings (e.g. Figure 5) and intense radiative forcing in the northern tropics and subtropics. Each simulation was forced with a representative strong dust forcing, as shown in Figure 20, crafted by Amato Evan. To generate this forcing, he used the Advanced Very High Resolution Radiometer (AVHRR) Pathfinders Atmospheres - Extended (PATMOS-x) satellite-based estimates of dust

aerosol optical depth (DAOD) from 1982-2010 (Evan and Mukhopadhyay 2010). He removed the DAOD seasonal cycle and made a June-August (JJA) averaged time series spanned over the region of 0-30°N and 15-65°W for DAOD. That averaged time series was used to select the four most and four least dusty years for JJA, which corresponded to the years with a positive or negative 1-sigma DAOD event. Lastly, the DAOD fields for the positive years were averaged and likewise for the negative years, before they were differenced (positive minus negative years). This gave a monthly dust forcing that was then used in the primary set of ensembles, as shown in Figure 20. For the sensitivity experiments, the second and third set of ensembles, half and then the negative of this forcing were used, respectively, to test linearity.

The dust aerosol radiative forcing that was used in the model simulations is shown in Figure 20. The forcing was applied to the model in the form of a modified Q-flux, as presented in Equation 1, and represents a reduction in downward radiation due to a dust outbreak. Figure 20 shows that years with excessive dust outbreaks are generally associated with a reduction in downward solar radiation at the surface (radiative forcing is nearly always negative). Negative dust radiative forcing begins off the west cost of North Africa in May, between around 5°N and 30°N. This forcing remains negative in the northern tropical Atlantic (between 5° - 30°N) through September, with maximum negative forcing occurring during June, July, and August. By October through November, dust radiative forcing is very weak, and by December the forcing is set to zero.

To investigate the response due to this forcing, the difference between the ensembles and the control were computed.  To do so, all of the years of the control were averaged to generate a 12 month climatology spanning April through the following May.  Similarly, all of the ensemble members for each set were averaged together to create a 12 month dust forced component.  To determine which differences are statistically significant, t-tests were performed.
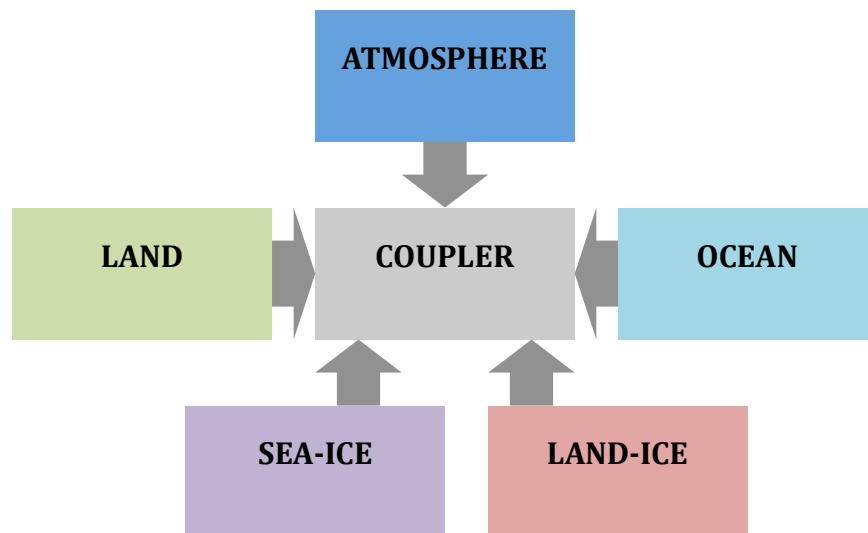
Figure 18. National Center for Atmospheric Research (NCAR) Community Earth System Model (CESM) five components working simultaneously through a central coupler.

Table 1. Breakdown of model runs performed for this study.

| NAME | TYPE | FORCING | LENGTH | INITIALIZATION |
|---|---|---|---|---|
| e2000control | Control | None | 50 years | Arbitrary |
| e2000branch | Branch | Full Dust Forcing | 40 ensemble members | From control; Years 10-49 |
| e2000branch.half | Branch | Half Dust Forcing | 20 ensemble members | From control; Years 10-29 |
| e2000branch.neg | Branch | Negative Dust Forcing | 20 ensemble members | From control; Years 10-29 |
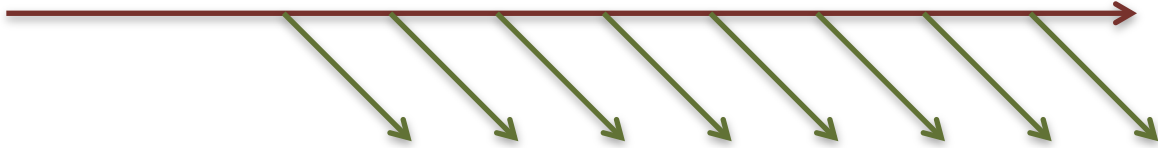
Figure 19.  Visualization of model runs, where the control run (dark red) is a continuous run and each branch run (green) is initialized at some point of the control run.
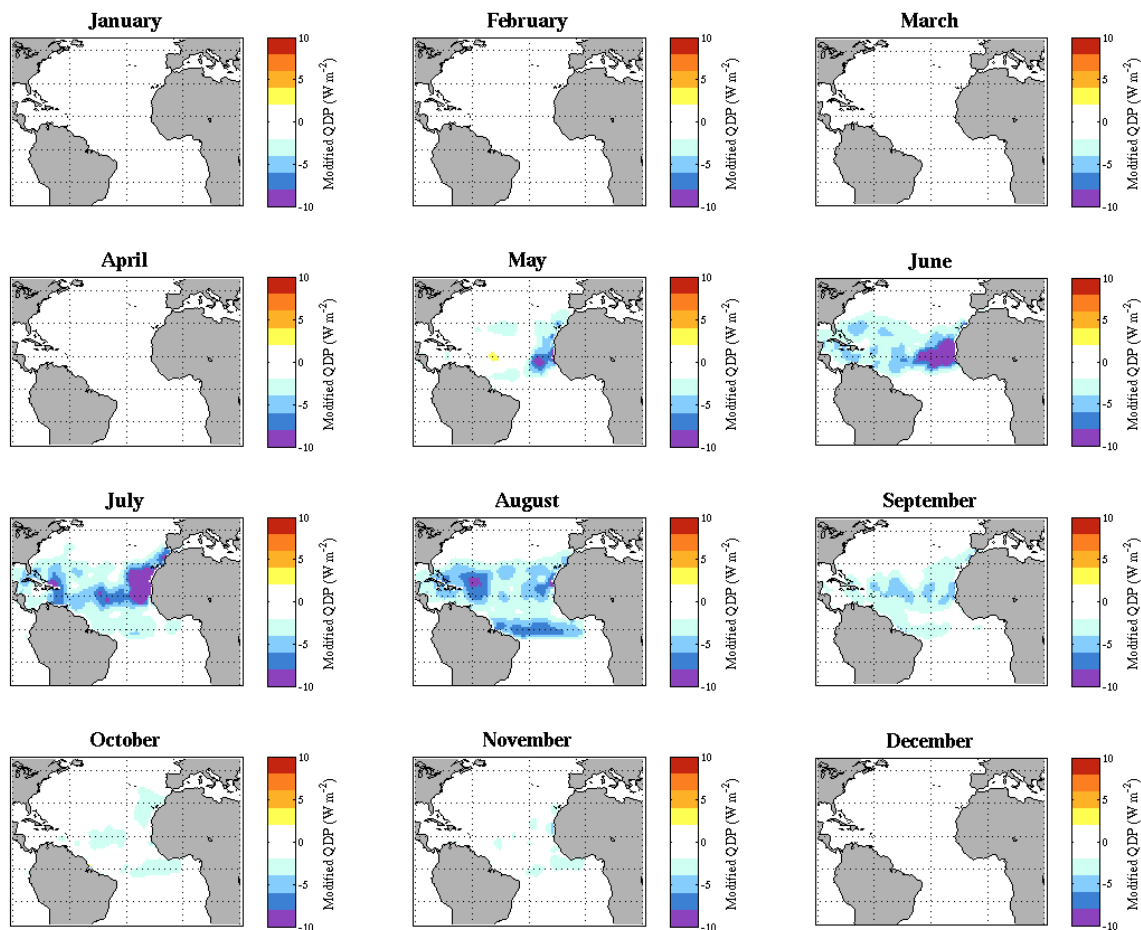


Figure 20. Modified Q-flux used to represent the dust outbreak forcing in the branch simulations.

## 3. RESULTS

This section will explore the results from the dust forced model simulation, the mechanism behind the response, and the sensitivity studies performed.

*a. Response to Dust*

The response of SST to imposed dust forcing in the e2000branch simulations is shown in Figure 21. The response begins to show a significant cold anomaly in June, just off the western coast of Africa, consistent with the dust radiative forcing during May and June. That cold response soon spreads westward across the tropical Atlantic between about 5-30°N and bears some resemblance to the AMM SST structure in the deep tropics. The cold anomalies in the northern tropical Atlantic persist through November, when the imposed forcing is shut off. From December through the following March, the cold anomalies in the northern tropical Atlantic appear to propagate westward and equatorward despite the fact that the forcing has been shut off. In addition to the cold anomalies that evolve in the northern tropical Atlantic, a warm anomaly is present in the southern subtropics around 25°S during November, December, and January. A secondary significant warm anomaly centered around 5-10°S emerges during January and February that will be discussed further below.

Figure 22 shows again the sea surface temperature response to dust, but also includes the difference in low level winds between the control and dust forced ensemble set. Results are shown for every other month, and wind vectors are

plotted only where significant at the 80% confidence level according to a bivariate t-test.  During January, an enhancement of the climatological easterlies exists north of the equator, between 5-15°N, while a slight reduction of the winds is present just south of the equator, between 0-10°S.  As shown earlier, the SST response is most robust just off the western coast of Africa, with negative SST anomalies centered around 15°N, in July and September.  Toward the end of the simulation, the cold anomaly propagates toward the equator.  A slight dipole structure exists from January to March, centered at the equator with a cool anomaly north of the equator and slight warm anomaly south of the equator.

The change in precipitation rate in the dust forcing run is shown in Figure 23.  A strong response in the intertropical convergence zone (ITCZ) is present, beginning to show up as early as July, but becoming more and more distinct toward the end of the simulation (i.e. January to March).  The ITCZ appears to shift southward in response to the dust forcing, with a reduction in the precipitation rate just north of the climatological ITCZ location and an increase in the precipitation rate south of the climatological ITCZ in the tropical Atlantic.  Interestingly, a very strong precipitation response lasts in the months after the forcing is shut off.  In fact, the precipitation response in the ITCZ region is stronger and more significant January through March than in earlier months.  As the precipitation response propagates westward and equatorward, it causes an increase in precipitation over the Nordeste region of Brazil, which is the far northeastern corner of Brazil, and a reduction in

precipitation across the equatorial region of South America. This response over land is strongest in January and March, centered around the equator.

The next plot, Figure 24, shows the change in sea level pressure between the dust forced ensemble set and climatology. Not much of a sea level pressure response exists due to dust forcing. The only significant response is during May, July, and January. The May and January response is an intensification of the subtropical high; while in July there is a large positive sea level pressure anomaly north of 30°N in the western mid-latitude Atlantic. It is worth noting that in January a large dipolar sea level pressure anomaly exists in the north Atlantic, centered around 35°N. The mid-latitude response could be forced by a teleconnection from the strong tropical precipitation response at that time, or it could be spurious, due to the fact that the mid-latitudes are particularly energetic during that season. The mid-latitude response does show up independently in both halves of the branch simulation.

As mentioned earlier, one of the responses to the imposed dust forcing includes an enhancement of the climatological easterly winds (an increase in wind speed) north of the equator and a slight reduction of the climatological easterly winds (a reduction in wind speed) just south of the equator. The 10 meter wind speed is shown in Figure 25. Throughout most of the simulation, an increase in the wind speed occurs just north of the equator, with a negative wind speed anomaly near the equator. The response is most apparent during January, where a dipole structure is center around the equator off the eastern coast of South America. The

changes in wind speeds play a very important role in the propagation of the

temperature response, which will be discussed further in Section 3b.

In this simulation, the evolution of SST is affected by the direct dust radiative

forcing (Figure 20), and the resulting surface heat flux, which is composed of the

latent, sensible, net shortwave, and net longwave heat fluxes (the sign convention is

such that upward heat flux anomalies are positive).  The sensible and net longwave

heat fluxes are negligible (not shown).  The latent heat flux response is shown in

Figure 26.  The first major feature to note is the negative anomaly off the western

coast of Africa, around 15°N, in the same region where SST shows a large cold

response.  The negative heat flux anomaly indicates a decrease in evaporation, and a

damping of the SST anomaly.  This reduction in evaporation in July through

September just off the western coast of Africa occurs where the dust forcing

response is the greatest and also where the location of the strongest cold anomaly in

sea surface temperature exists.  The second feature to note is the dipole of latent

heat flux on either side of the equator, present through most of the simulation.  An

increase in the latent heat flux (i.e. increase in evaporation) is present just north of

the equator early on in the simulation, while a decrease in latent heat flux is present

near the equator.  This dipolar latent heat flux shows up occasionally, but is most

robust in January. The latent heat flux response will also be discussed further in

section 3b.

The net solar heat flux is shown next in Figure 27.  Throughout the first half

of the simulation, a slight reduction in the net solar heat flux exists across the

tropics. Toward the end of the simulation, a distinct increase in the solar heat flux is shown just south of the equator, extending over the Nordeste region of Brazil, with a slight decrease in the solar heat flux just to the north near the equatorial region. Overall, the solar heat flux response is much more noisy than the latent heat flux (which is already somewhat noisy), but does appear to follow the precipitation variations in the tropical regions.

Figure 28 shows the net surface heat flux, calculated as the sum of the shortwave, longwave, latent and sensible heat fluxes. A significant reduction in the net surface heat flux is occurs July through September off the coast of the Sahara, where the forcing is primarily located. This reduction is primarily due to a decrease in evaporation, as shown in the latent heat flux maps in Figure 26. In November, a positive anomaly in the net surface heat flux shows up in the north central equatorial region, around 30°W. That positive net heat flux response propagates westward and southward throughout the next months, and is particularly evident during January off the east coast of Brazil.

*b. Mechanism*

As presented in the previous section, the response due to the dust forcing is located in the region of where the forcing was applied, but also extends outside the spatial region of forcing. In addition, it continues its propagation through the boreal winter months, beyond the time when the forcing is shut off. This section will investigate the process driving this response.

The bulk formula for latent heat flux can be written as (Vimont 2010):

$$LH = L_v C_e \rho_a |\vec{u}| \left( q_{sat}(T_s) - RH \cdot q_{sat}(T_{a,ref}) \right) \qquad (2)$$

The two components of the latent heat flux that we will be investigating in this study include changes in the vertical moisture gradient, $q_{sat}$, and changes in wind speed, $|\vec{u}|$. Typically, when the water surface temperatures are cold, it is expected that there is less evaporation (i.e. less upward latent heat flux) due to a reduction in the vertical moisture gradient near the surface. Due to the exponential nature of the Clausius-Clayperon relationship and the fact that near-surface air temperature is typically less than surface temperature, a reduction in temperature reduces the vertical moisture gradient, which reduces evaporation. Looking back at Figure 22, a cold anomaly exists due to dust off the western coast of Africa, centered at around 15-20°N. A reduction in the latent heat flux also is present in the same region.

We have monthly estimates of $|\vec{u}|$ and of the latent heat flux. On monthly time scales, the sub-monthly covariance between $|\vec{u}|$ and the vertical moisture gradient will affect the sensitivity of the latent heat flux to variations in wind speed. However, as shown by Smirnov and Vimont (2011) these variations can largely be ignored. As such, we approximate the wind speed contribution to the latent heat flux anomaly as:

$$\Delta LH = \overline{LHFLX} \cdot \frac{\Delta |\vec{u}|}{|\vec{u}|} \qquad (3)$$

where $|\vec{u}|$ and $\overline{LHFLX}$ are the climatological wind and latent heat flux from the control simulation, and $\Delta |\vec{u}|$ is the difference between the dust-forced simulation and the control simulation.

It has been shown that the AMM is characterized by a SST gradient that includes winds that blow towards warmer water and veer to the right in the northern hemisphere and to the left in the southern hemisphere (Chiang and Vimont 2004). This leads to a relaxation of winds over warm water and an intensification of winds over cold water, resulting in a positive feedback on the original SST gradient through change of evaporation (i.e. latent heat flux). This feedback is referred to as the wind, evaporation, SST, or WES feedback (Chang et al. 1997). We examine the contribution of the WES feedback to the evolution of SST in the dust forced simulation by investigating the wind speed contribution to the latent heat flux.

As described, the latent heat flux was decomposed by looking at the wind speed contribution to latent heat flux. First, Figure 29 shows the fractional change in wind speed. A relaxation in the wind speeds shows up early on in the model simulation. Remembering that the forcing was applied beginning in April and increased in intensity throughout June, July, and August, before weakening through September, October, and November, a coupling between an enhancement and relaxation of the westerlies shows up in July. That dipole structure, located along the equator, becomes more and more pronounced throughout the entire simulation.

Figure 30 shows the contribution of wind speed to the latent heat flux. Warm colors in Figure 30 indicate a strong contribution of wind speed to latent heat flux anomalies. Comparing to Figures 25 and 26, the 10 m wind speed and the latent heat flux, regions of intensified wind speeds correspond to regions of increased

evaporation. The reverse is true of the cool colors, where those correspond to regions of relaxed wind speeds and reduced evaporation. It is interesting to note that this dipole structure in Figure 30 extends into the months after the forcing is removed. In fact, the wind speed contribution to latent heat flux is greatest in January and March, at the end of the simulation. In addition, other coupled features in this figure show up in the subtropics, outside of the spatial region of the forcing. These features require further investigation. The most interesting feature, however, is the coupled response tightly confined to the equator, that propagates westward and equatorward throughout the simulation. Typically, it is expected to find a reduction in latent heat flux over regions of cold water and over warm water, to have increased latent heat flux. In this case, that is not the case, and an intensification of the winds leading to an increase in evaporation is collocated with the cold anomaly, while a relaxation of the winds leading to a reduction in evaporation is collocated with the warm anomaly. Therefore, the winds in those regions play an important role in this response and in the propagation of the SST response due to dust.

*c. Sensitivity Experiments*

In order to ensure the validity of the results and check for linearity, two additional ensemble sets of model runs were performed. The first contained half the amplitude of the original dust forcing, while the second contained the opposite amplitude of the original forcing. Each set had 20 ensembles members, instead of

40 members like the original ensemble set.  Each simulation was 12 months long, beginning in April 1st years 10 through 29, as stated in Table A.  The same control simulation was used in creating a 12 month climatology, but only the corresponding 20 years were used in creating the control record.  In the same way as the original ensemble set, the difference between the ensembles and the control were computed and t-tests were performed to determine which differences are statistically significant.

*i. Half dust forcing*

When forcing the model with only half the amplitude of the dust forcing in comparison to the full dust forcing used originally, little change was found in the response.  Figures 31, 32, and 33 are difference plots when the half dust forcing was used.  Figure 31 shows the SST and wind response from this experiment.  The scale is the same as Figure 21, which shows the SST response to the original dust forcing.  Note a similar cold anomaly is present in June and intensifies through July, August, and September off the coast of western Africa.  As time continues, it propagates westward and equatorward, very similar to the original response.  Figure 32 presents the precipitation rate response from the half dust forcing.  A very similar coupled ITCZ structure shows up here, beginning to develop early on in the response in the tropics.  Similar to the SST response, it propagates westward and equatorward with time.  This dipole structure of reduction and intensification of precipitation rate extends beyond the forcing being shut off and over a large portion of South America.  In comparison with Figure 23, which shows the precipitation rate

response to the original dust forcing, the southward shift of the ITCZ is consistent,

with an increase of precipitation over the Nordeste region of Brazil. The latent heat

flux response to this half dust forcing is a very large response and even more robust

than the response to the original forcing. Throughout the entire simulation, wind

speeds are playing a large role in the propagation of the SST anomalies. The WES

feedback appears to be driving the response in this experiment as well; with

reduction in wind speeds and reduced evaporation collocated with warm SST

anomalies while intensification in wind speeds and increased evaporation is

collocated with cold anomalies.

### ii. Opposite dust forcing

In addition to forcing the model with half the amplitude of forcing, a second

set of sensitivity studies was performed, where the opposite sign of the original

forcing was applied to check for linearity. Changing the sign did not produce a

linear response. Figures 34, 35, and 36 show the difference plots when the opposite

forcing was used. The response is far less consistent with the original forcing than

the half forcing result. In the first half of the simulation, a distinct warming occurs

just off the western coast of the Sahara, in the same region as the cold anomaly was

located during the original simulation. During the latter half of the simulation, there

are scattered warm anomalies both in the northern and southern subtropics.

Especially in the second half of the simulation, the equatorial region remains

unchanged with respect to the control simulation. The precipitation response is

quite irregular, but is in fact, showing some of the same features as the original

forcing result, including a very slight southward ITCZ shift during the last couple months of the simulation.  Especially during the first half of the response, the precipitation response is mainly confined to the northern equatorial region.  Lastly, no distinct intensification or reduction of the winds in the equatorial region exists.  There are, however, wind speed changes in the subtropics extending toward the midlatitudes.  The increases in wind speeds are collocated with latent heat flux amplifications, while the areas of weakening wind speeds are located over regions of latent heat flux reduction.  This corresponding relationship shows that the winds are playing a substantial role in this response, as in the original and half forcing simulations.

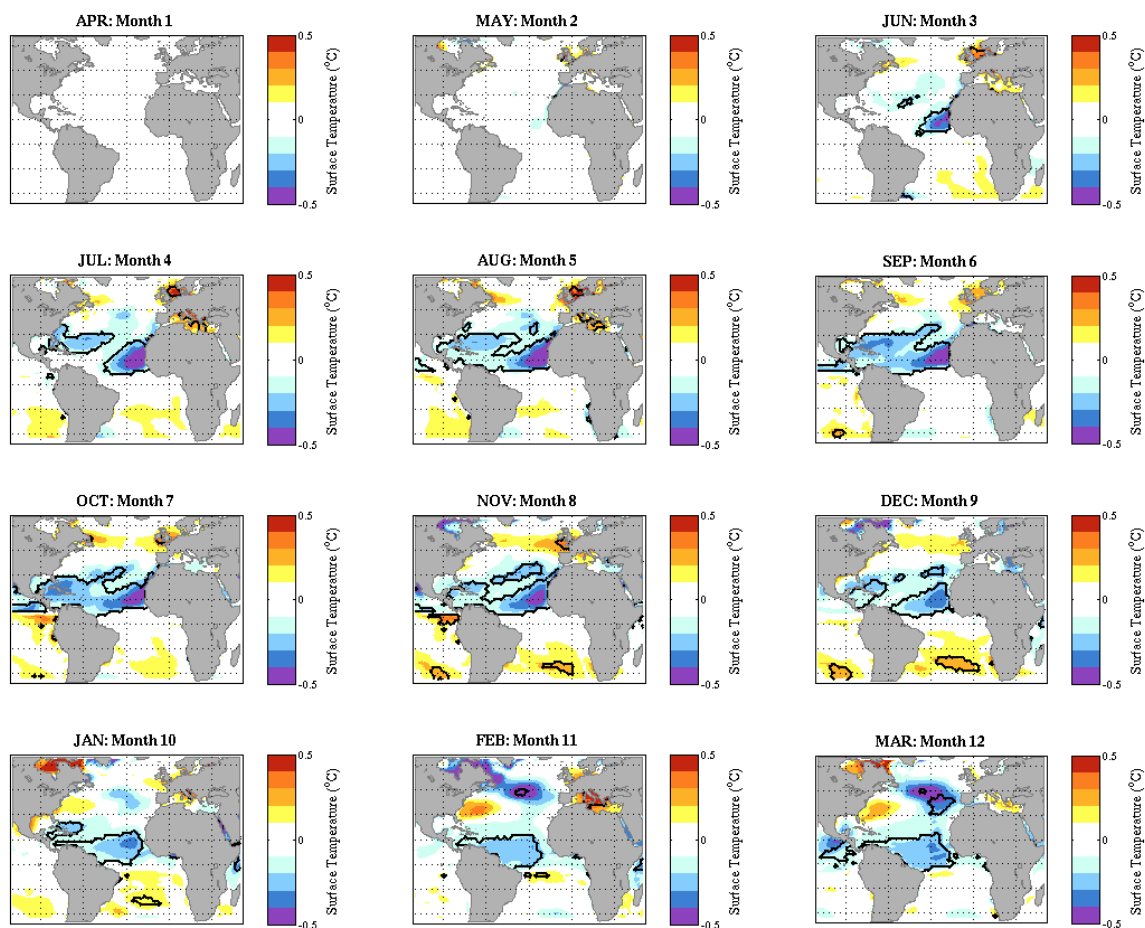Figure 21. Sea surface temperature (°C) difference due to dust forcing. Black line indicates where response is statistically significant at the 95% confidence level.



Figure 22. Sea surface temperature (°C) and wind vector difference due to dust forcing.

Figure 23. Precipitation rate (mm/day) difference due to dust forcing. Black line indicates where response is statistically significant at the 95% confidence level.
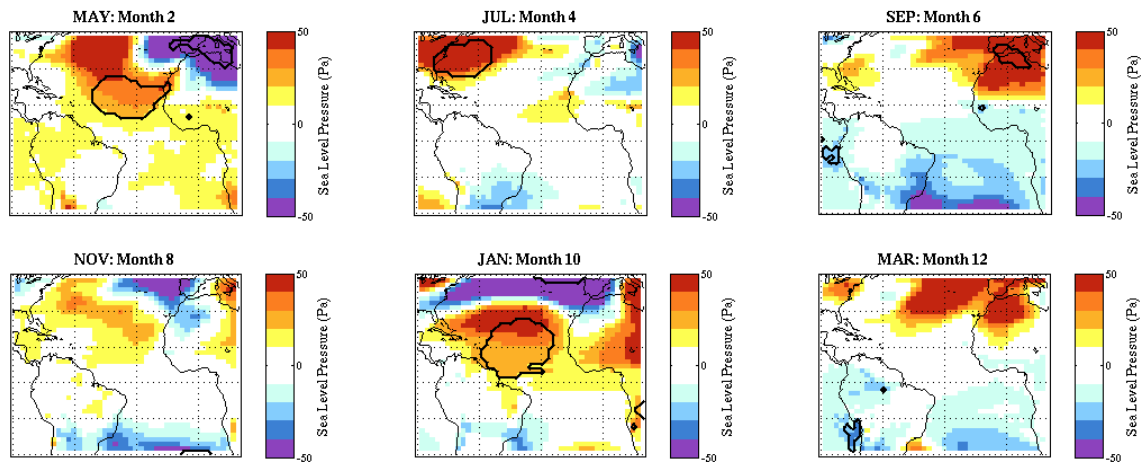


Figure 24. Sea level pressure (Pa) difference due to dust forcing. Black line indicates where response is statistically significant at the 95% confidence level.
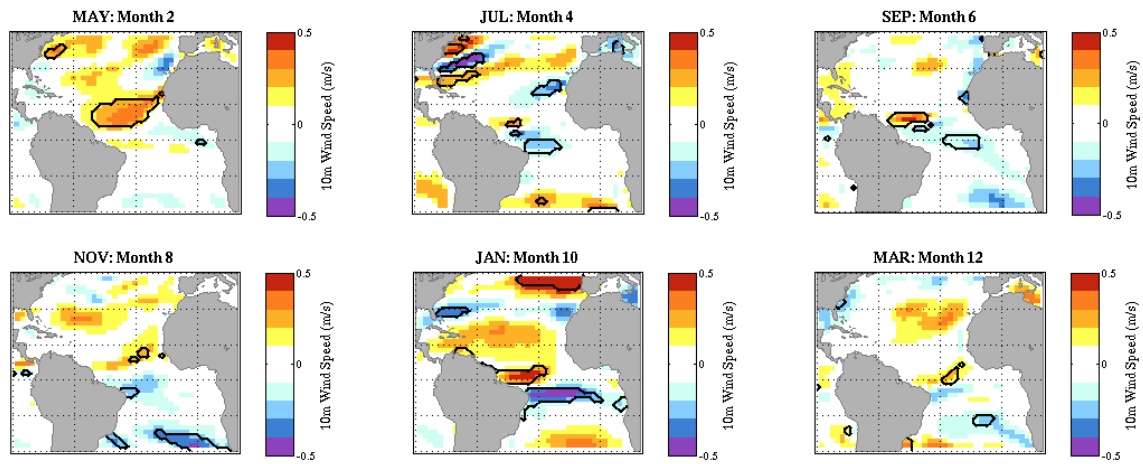
Figure 25. 10 meter wind speed (m/s) difference due to dust forcing. Black line indicates where response is statistically significant at the 95% confidence level.
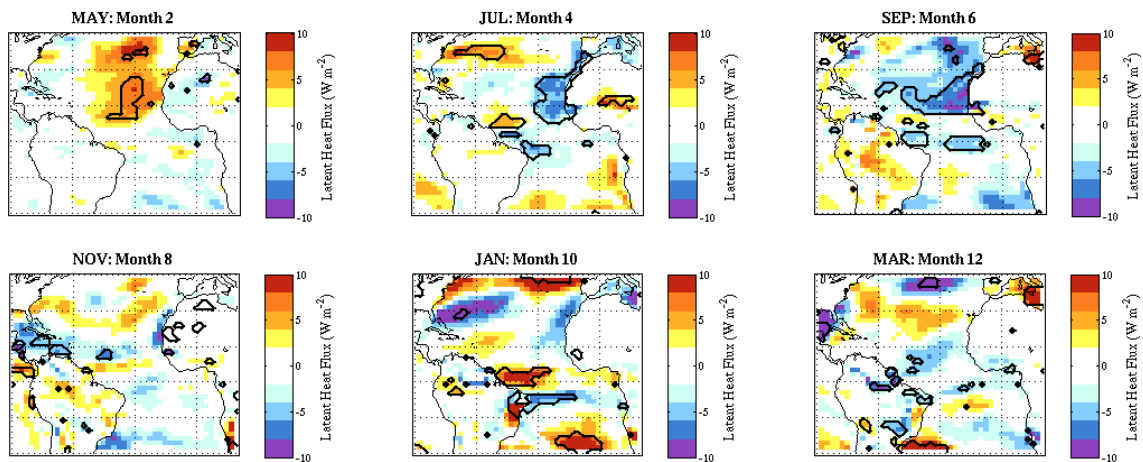


Figure 26. Latent heat flux (W m$^{-2}$) difference due to dust forcing. Black line indicates where response is statistically significant at the 95% confidence level.
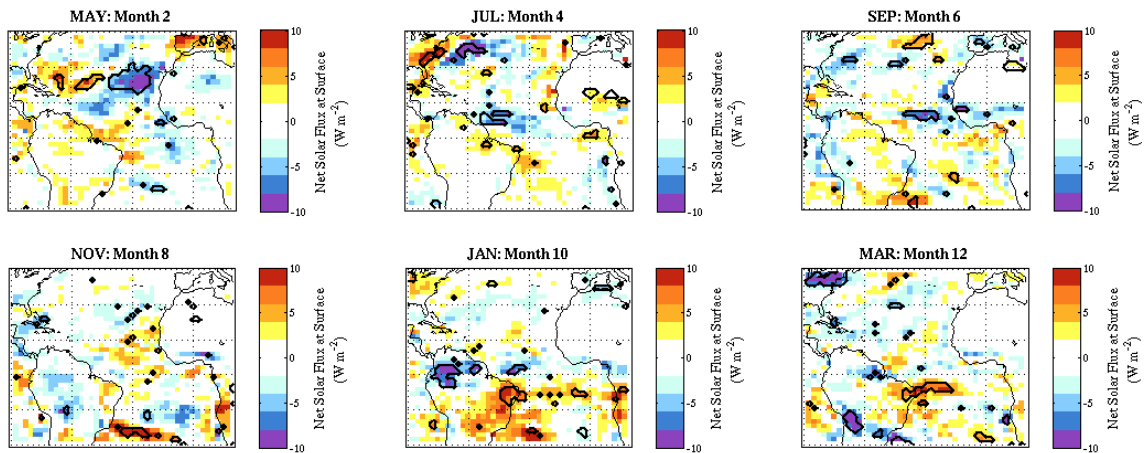
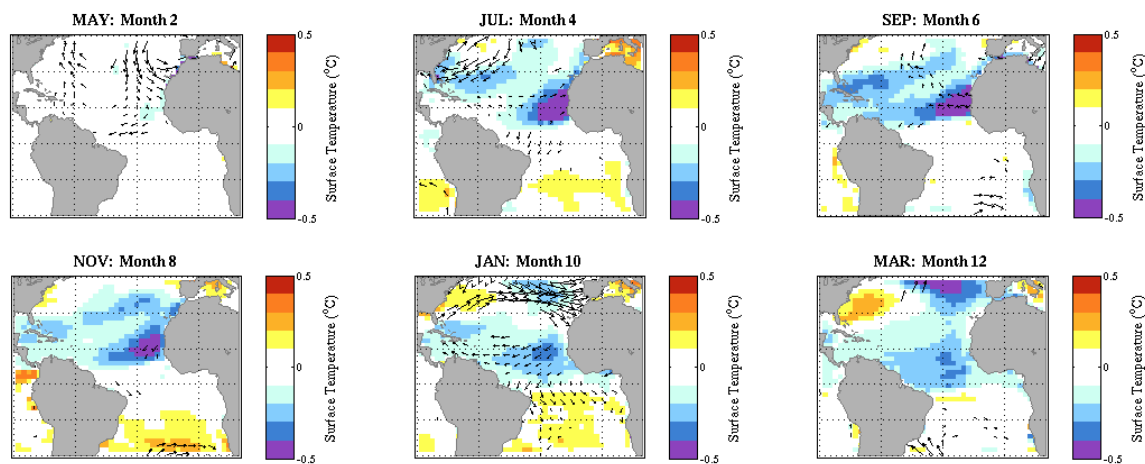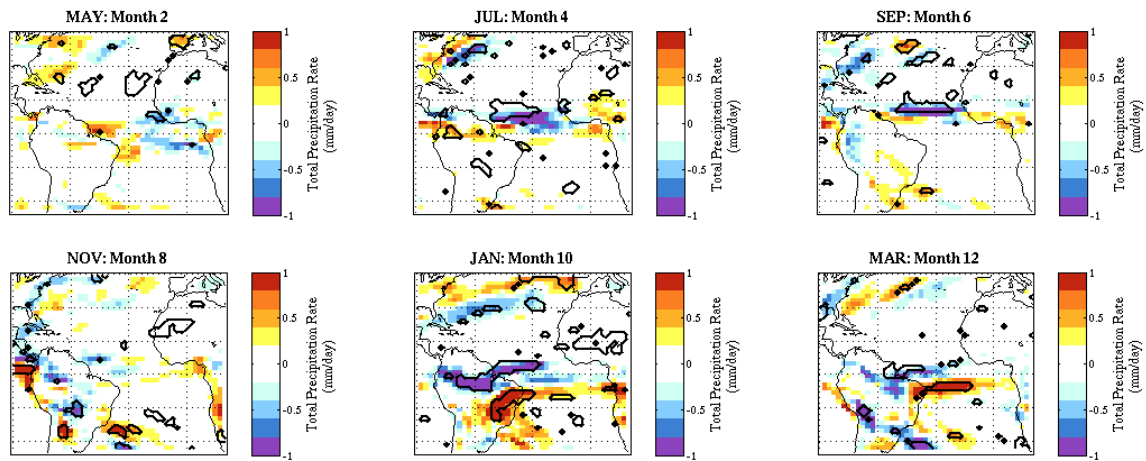Figure 27. Net solar heat flux (W m$^{-2}$) difference due to dust forcing. Black line indicates where response is statistically significant at the 95% confidence level.
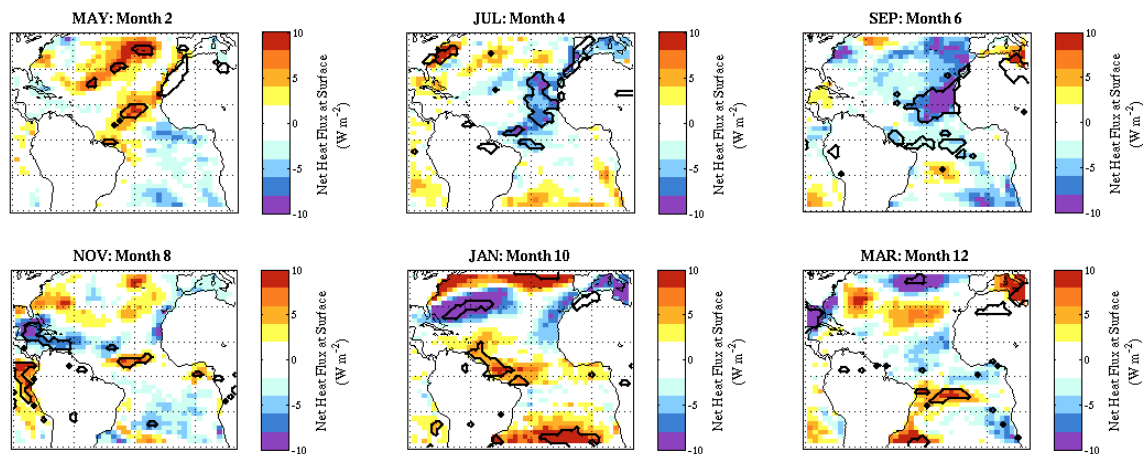


Figure 28. Net surface heat flux (W m$^{-2}$) difference due to dust forcing. Black line indicates where response is statistically significant at the 95% confidence level.
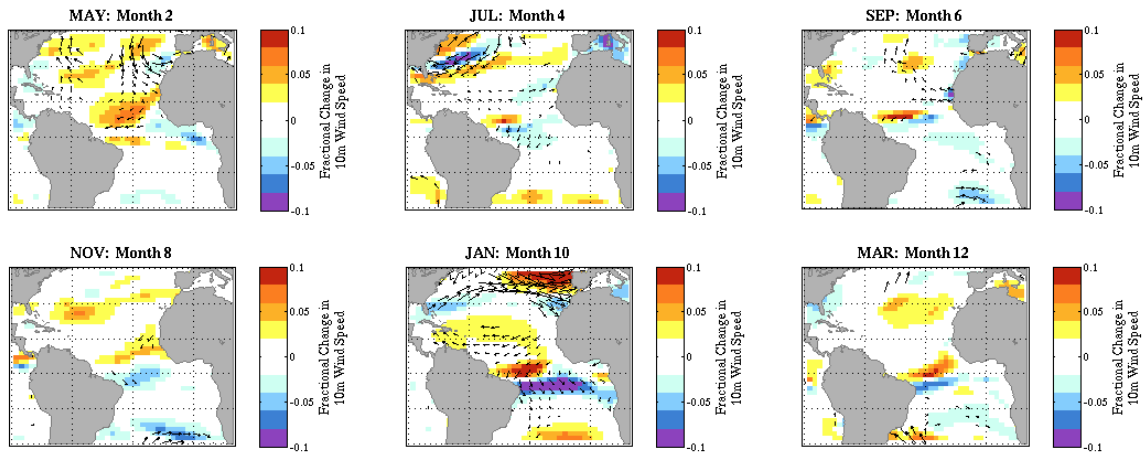
Figure 29. Fractional change in 10 m wind speed (shaded) and wind direction change (vectors).
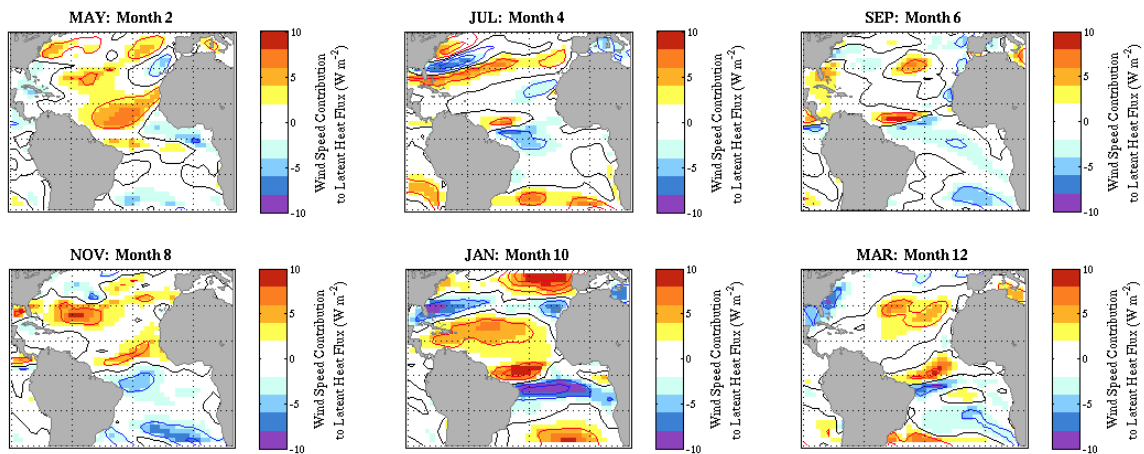


Figure 30. Wind speed contribution to latent heat flux (W m-2).  Red (blue) contours are increases (decreases) in wind speeds.
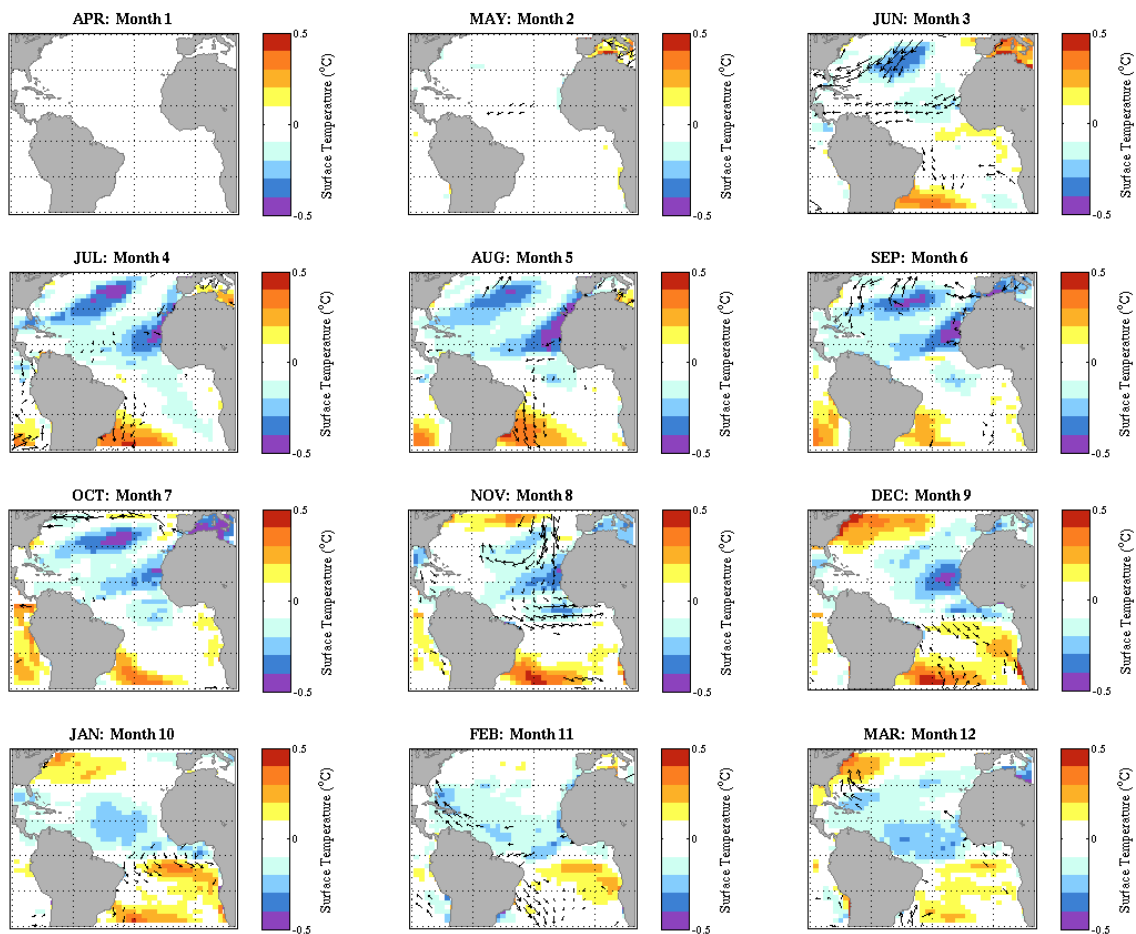
Figure 31. Sea surface temperature (°C) and wind vector difference from the half dust forcing experiment.
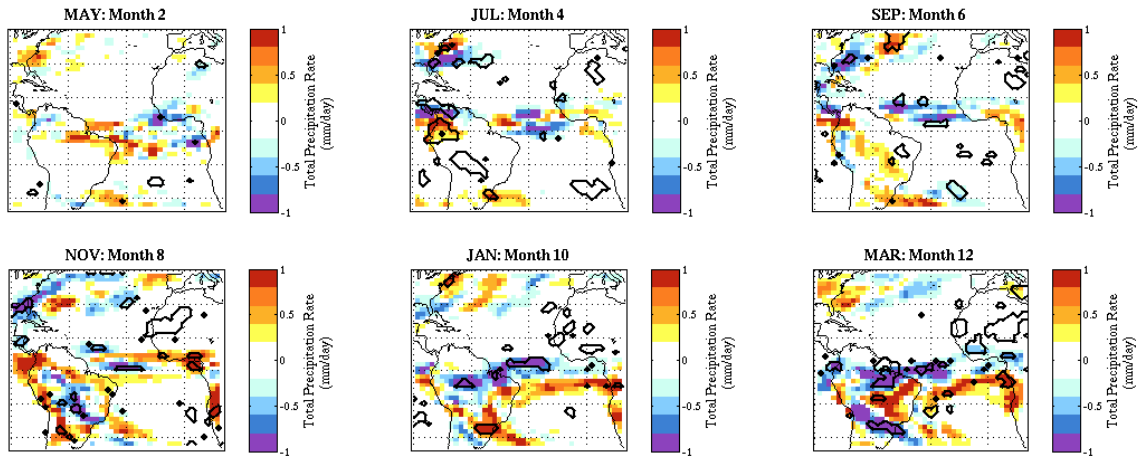
Figure 32. Precipitation rate (mm/day) difference from the half dust forcing experiment. Black line indicates where response is statistically significant at the 95% confidence level.
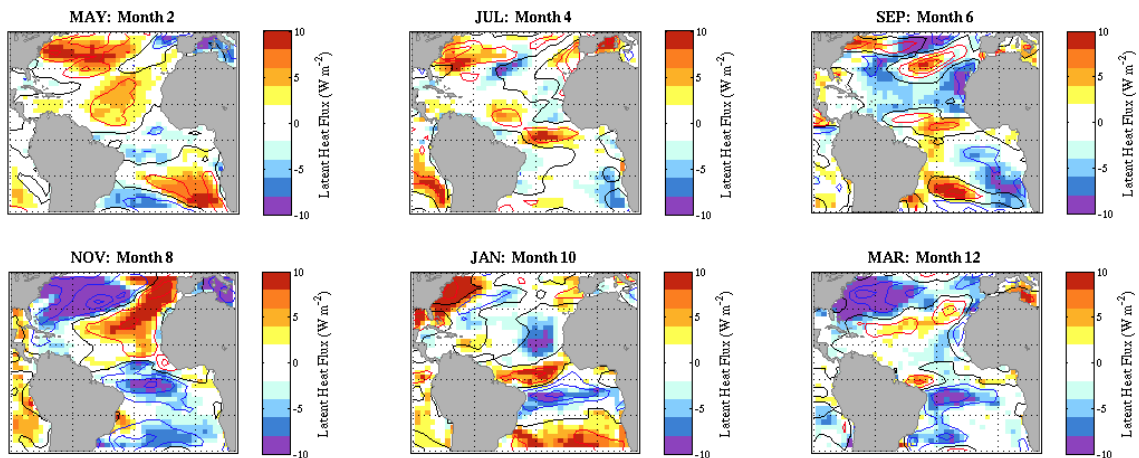


Figure 33. Latent heat flux (W m$^{-2}$; shaded) and 10m wind speed (contours) difference from the half dust forcing experiment. Red (blue) contours are increases (decreases) in wind speeds.
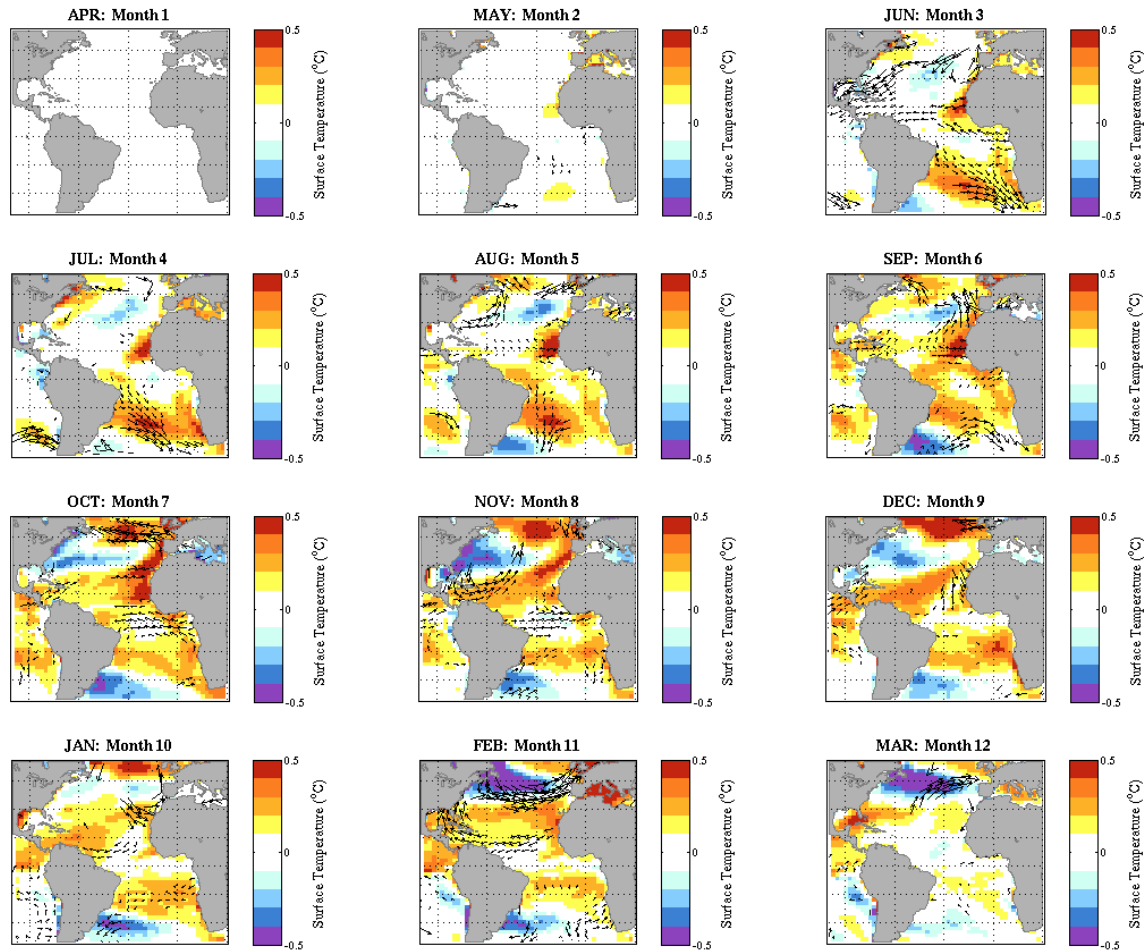
Figure 34. Sea surface temperature (°C) and wind vector difference from the opposite dust forcing experiment.
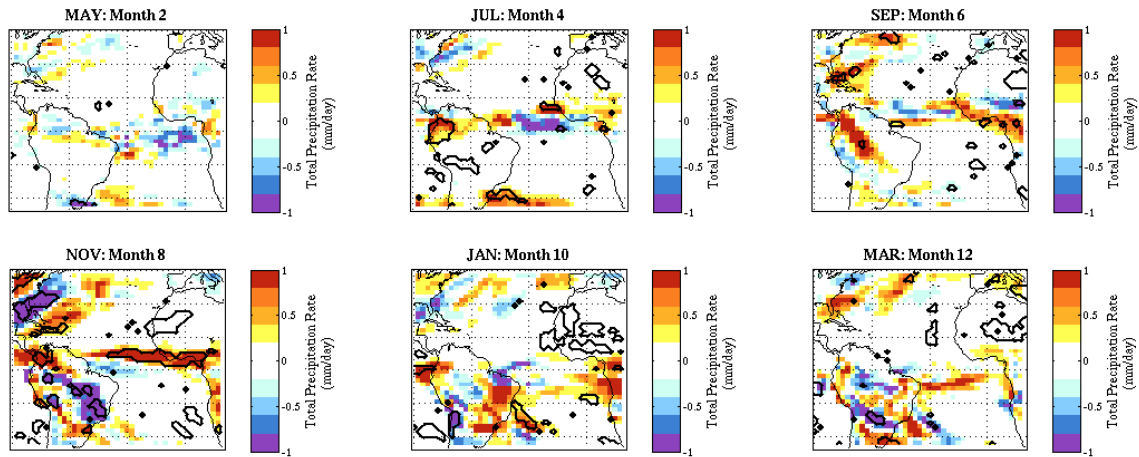
Figure 35. Precipitation rate (mm/day) difference from the opposite dust forcing experiment. Black line indicates where response is statistically significant at the 95% confidence level.
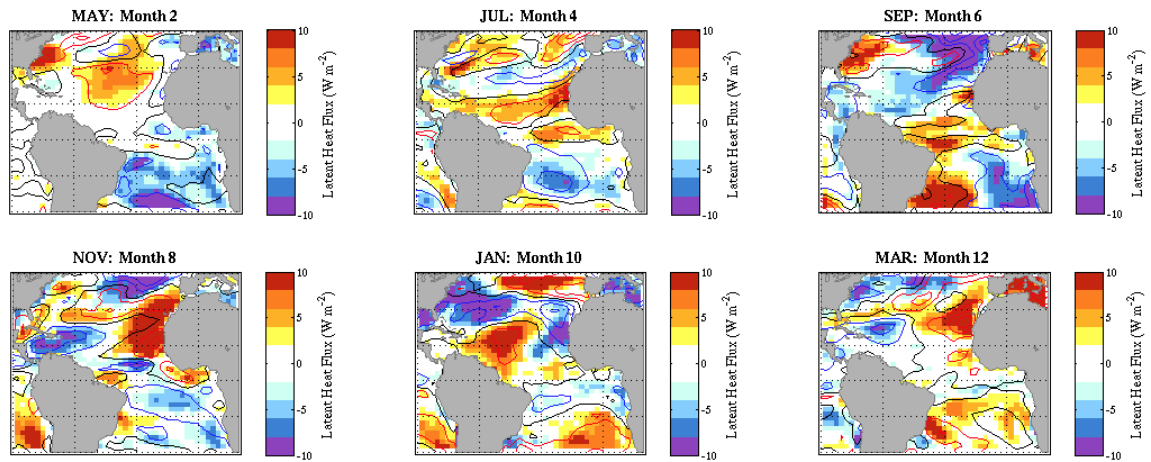


Figure 36. Latent heat flux (W m⁻²; shaded) and 10m wind speed (contours) difference from the opposite dust forcing experiment. Red (blue) contours are increases (decreases) in wind speeds.

## 4. CONCLUSIONS AND DISCUSSION

*a. Conclusions*

Previous research shows that African dust has an impact on SST in the tropical North Atlantic Ocean. Even et al. (2011) had explored the response of a dust forcing in an idealized coupled model. In the present study, a fully coupled model was used to investigate the coupled feedback and processes due to a dust forcing. A control model simulation and an ensemble set of simulations were performed to investigate this dust response. In addition, two sensitivity ensemble sets of ensembles were performed to check for linearity.

Two major features were found in performing this experiment. A strong direct response of cooler SSTs was present off the western coast of Africa. This feature works to generate the negative phase of the AMM. The tropical response extends several months after the forcing event is over and is present in regions that are not directly forced by the dust. Further, an indirect response occurred due to coupled ocean-atmosphere processes in the model, including changes in wind and a large shift of the ITCZ during boreal winter. The ITCZ appears to shift southward and extend over land, causing an increase in precipitation over the Nordeste region of Brazil. The mechanism identified to be responsible for the westward and equatorward evolution of this tropical response is the WES feedback.

Two sensitivity experiments were performed to investigate the linearity of the response: the first experiment used half the amplitude of the original dust forcing, and the second used the opposite polarity of the original dust forcing. The model with only

half the amplitude of the dust forcing reproduced similar results as that of the original simulation. The model with the negative forcing did not produce linear results. This response was far less consistent with the original forcing than the half forcing result, in that the response was widespread and irregular.

*b. Discussion and Future Work*

The most obvious implications of this dust forced tropical response include the displacement of the ITCZ and changes in the precipitation pattern in the tropics, primarily South America. This study also supports previous work that has identified a significant response due to African dust in the tropics.

Some caveats to note with this experiment include that this only explores the direct response to forcing in a fully coupled model, not the indirect response to cloud microphysics, aerosols, etc., which may have a significant effect. Also, this experiment only forces the model at the surface and changes in the whole atmosphere heating rate may affect the response. Lastly, as with any model, biases exist.

To further this study, many paths exist. An important next step is to check for observational consistency to see if the same variations are present in nature. Composite analysis of dust outbreaks can be performed and long-term records of precipitation in Brazil can be compared with the precipitation result found. It is worth investigating whether the response of the ITCZ is due to the change in SST or due to the coupled response in the tropics. A way to do this would be to check the

ITCZ response in an uncoupled model. Another point of interest is to understand better the mid-latitude response and whether or not that response is a realistic teleconnection to the tropical response. It would also be interesting to look at the time evolution of the dust forcing. Lastly, it is key to broadly understand if the results from this experiment imply any useful predictability.

## REFERENCES

BBC. 2012. "Geography: Drought." *GCSE Bitesize Geography*.

http://www.bbc.co.uk/schools/gcsebitesize/geography/water_rivers/drought

_rev3.shtml.

Bailey, David, Cecile Hannay, Marika Holland, and Richard Neale. 2010. *Slab Ocean

Model Forcing*. www.cesm.ucar.edu/models/ccsm4.0/data8/SOM.pdf.

Bitz, C. M., K. M. Shell, P. R. Gent, D. Bailey, G. Danabasoglu, K. C. Armour, M. M.

Holland, and J. T. Kiehl. 2011. "Climate Sensitivity of the Community Climate

System Model Version 4." *Journal of Climate* (December 8): 111209062051003.

doi:10.1175/JCLI-D-11-00290.1.

http://journals.ametsoc.org/doi/abs/10.1175/JCLI-D-11-00290.1.

Chiapello, Isabel, Cyril Moulin, and Joseph M. Prospero. 2005. "Understanding the

Long-term Variability of African Dust Transport Across the Atlantic as

Recorded in Both Barbados Surface Concentrations and Large-scale Total

Ozone Mapping Spectrometer (TOMS) Optical Thickness." *Journal of

Geophysical Research* 110 (D18): 1–9. doi:10.1029/2004JD005132.

http://www.agu.org/pubs/crossref/2005/2004JD005132.shtml.

Dunion, Jason P., and Christopher S. Velden. 2004. "The Impact of the Saharan Air

Layer on Atlantic Tropical Cyclone Activity." *Bulletin of the American*

*Meteorological Society* 85 (3) (March): 353–365. doi:10.1175/BAMS-85-3-353.
http://journals.ametsoc.org/doi/abs/10.1175/BAMS-85-3-353.

Evan, Amato T, Daniel J Vimont, Andrew K Heidinger, James P Kossin, and Ralf
Bennartz. 2009. "The Role of Aerosols in the Evolution of Tropical North
Atlantic Ocean Temperature Anomalies." *Science (New York, N.Y.)* 324 (5928)
(May 8): 778–81. doi:10.1126/science.1167404.
http://www.ncbi.nlm.nih.gov/pubmed/19325076.

Evan, Amato T., Jason Dunion, Jonathan a. Foley, Andrew K. Heidinger, and
Christopher S. Velden. 2006. "New Evidence for a Relationship Between
Atlantic Tropical Cyclone Activity and African Dust Outbreaks." *Geophysical
Research Letters* 33 (19) (October 10): 1–5. doi:10.1029/2006GL026408.
http://www.agu.org/pubs/crossref/2006/2006GL026408.shtml.

Evan, Amato T., Gregory R. Foltz, Dongxiao Zhang, and Daniel J. Vimont. 2011.
"Influence of African Dust on Ocean–atmosphere Variability in the Tropical
Atlantic." *Nature Geoscience* 4 (11) (October 2): 762–765.
doi:10.1038/ngeo1276.
http://www.nature.com/doifinder/10.1038/ngeo1276.

Evan, Amato T., Andrew K. Heidinger, Ralf Bennartz, Val Bennington, Natalie M.
Mahowald, Hector Corrada-Bravo, Christopher S. Velden, Gunnar Myhre, and
James P. Kossin. 2008. "Ocean Temperature Forcing by Aerosols Across the

Atlantic Tropical Cyclone Development Region." *Geochemistry Geophysics Geosystems* 9 (5) (May 29): 1–11. doi:10.1029/2007GC001774. http://www.agu.org/pubs/crossref/2008/2007GC001774.shtml.

Evan, Amato T., and Sujoy Mukhopadhyay. 2010. "African Dust over the Northern Tropical Atlantic: 1955–2008." *Journal of Applied Meteorology and Climatology* 49 (11) (November): 2213–2229. doi:10.1175/2010JAMC2485.1. http://journals.ametsoc.org/doi/abs/10.1175/2010JAMC2485.1.

Foltz, Gregory R., and Michael J. McPhaden. 2008a. "Impact of Saharan Dust on Tropical North Atlantic SST*." *Journal of Climate* 21 (19) (October): 5048–5060. doi:10.1175/2008JCLI2232.1. http://journals.ametsoc.org/doi/abs/10.1175/2008JCLI2232.1.

———. 2008b. "Trends in Saharan Dust and Tropical Atlantic Climate During 1980–2006." *Geophysical Research Letters* 35 (20) (October 25): 1–5. doi:10.1029/2008GL035042. http://www.agu.org/pubs/crossref/2008/2008GL035042.shtml.

Giannini, a, R Saravanan, and P Chang. 2003. "Oceanic Forcing of Sahel Rainfall on Interannual to Interdecadal Time Scales." *Science (New York, N.Y.)* 302 (5647) (November 7): 1027–30. doi:10.1126/science.1089357. http://www.ncbi.nlm.nih.gov/pubmed/14551320.

Holland, Greg J, and Peter J Webster. 2007. "Heightened Tropical Cyclone Activity in

the North Atlantic: Natural Variability or Climate Trend?" *Philosophical*

*Transactions. Series A, Mathematical, Physical, and Engineering Sciences* 365

(1860) (November 15): 2695–716. doi:10.1098/rsta.2007.2083.

http://www.ncbi.nlm.nih.gov/pubmed/17666389.

Husar, Rudolf B., Joseph M. Prospero, and Larry L. Stowe. 1997. "Characterization of

Tropospheric Aerosols over the Oceans with the NOAA Advanced Very High

Resolution Radiometer Optical Thickness Operational Product." *Journal of*

*Geophysical Research* 102 (D14): 16,889–16,909.

http://www.google.com/url?sa=t&rct=j&q=&esrc=s&source=web&cd=1&ved=

0CE4QFjAA&url=http%3A%2F%2Fwww.ewp.rpi.edu%2Fhartford%2F~ernest

o%2FSu2011%2FEP%2FMaterialsforStudents%2FRoberg%2FHusar1997.PDF

&ei=c9jQT8ObD6bF2QXz4-mqDA&usg=AFQjCNF0hJeLtZQcvy-Rdd-K59qvRw-

EeQ&sig2=hjdYvB9FnmOOCxSRwLecyA.

Kaufman, Yoram J, Ilan Koren, Lorraine a Remer, Daniel Rosenfeld, and Yinon

Rudich. 2005. "The Effect of Smoke, Dust, and Pollution Aerosol on Shallow

Cloud Development over the Atlantic Ocean." *Proceedings of the National*

*Academy of Sciences of the United States of America* 102 (32) (August 9): 11207–

12. doi:10.1073/pnas.0505191102.

http://www.pubmedcentral.nih.gov/articlerender.fcgi?artid=1182178&tool=p

mcentrez&rendertype=abstract.

Mahowald, Natalie M., and Chao Luo. 2003. "A Less Dusty Future?" *Geophysical Research Letters* 30 (17): 0–3. doi:10.1029/2003GL017880. http://www.agu.org/pubs/crossref/2003/2003GL017880.shtml.

Moulin, C. 2004. "Evidence of the Control of Summer Atmospheric Transport of African Dust over the Atlantic by Sahel Sources from TOMS Satellites (1979–2000)." *Geophysical Research Letters* 31 (2): 10–13. doi:10.1029/2003GL018931. http://www.agu.org/pubs/crossref/2004/2003GL018931.shtml.

NASA. 2008. "Saharan Dust Off West Africa." *Image of the Day Gallery*. http://www.nasa.gov/multimedia/imagegallery/image_feature_22_prt.htm.

Prospero, Joseph M. 2011. "Long Term Trends in African Dust Transport to the Caribbean: African Sources, Changing Climate, and Future Scenarios." In *First International Workshop on the Long-Range Transport and Impacts of African Dust on the Americas*, 1–84.

Prospero, Joseph M, and Toby N Carlson. 1972. "Vertical and Areal Distribution of Saharan Dust over the Western Equatorial North Atlantic Ocean." *Journal of Climate* 77 (27): 5255–5265.

Prospero, Joseph M, and Peter J Lamb. 2003. "African Droughts and Dust Transport to the Caribbean: Climate Change Implications." *Science (New York, N.Y.)* 302

(5647) (November 7): 1024–7. doi:10.1126/science.1089915.
http://www.ncbi.nlm.nih.gov/pubmed/14605365.

Prospero, Joseph M., Paul Ginoux, Omar Torres, Sharon Nicholson, and Thomas Gill.
2002. "Environmental Characterization of Global Sources of Atmospheric Soil
Dust Identified with the NIMBUS 7 Total Ozone Mapping Spectrometer (TOMS)
Absorbing Aerosol Product." *Reviews of Geophysics* 40 (1): 1–31.
doi:10.1029/2000RG000095.
http://www.agu.org/pubs/crossref/2002/2000RG000095.shtml.

Schollaert, Stephanie E, and John T Merrill. 1998. "Cooler Sea Surface West of the
Sahara Desert Correlated to Dust Events." *Geophysical Research Letters* 25 (18):
3529–3532.

Smirnov, Dimitry, and Daniel J. Vimont. 2011. "Variability of the Atlantic Meridional
Mode During the Atlantic Hurricane Season." *Journal of Climate* 24 (5) (March):
1409–1424. doi:10.1175/2010JCLI3549.1.
http://journals.ametsoc.org/doi/abs/10.1175/2010JCLI3549.1.

Tegen, I. 2004. "Relative Importance of Climate and Land Use in Determining
Present and Future Global Soil Dust Emission." *Geophysical Research Letters* 31
(5). doi:10.1029/2003GL019216.
http://www.agu.org/pubs/crossref/2004/2003GL019216.shtml.

Tegen, Ina, and Inez Fung. 1995. "Contribution to the Atmospheric Mineral Aerosol Load from Land Surface Modification." *Journal of Geophysical Research* 100 (D9): 18,707–18,726.

Vertenstein, Mariana, Tony Craig, Adrianne Middleton, Diane Feddema, and Chris Fischer. 2012. "CESM1.0.4 User's Guide." http://www.cesm.ucar.edu/models/cesm1.0/cesm/cesm_doc_1_0_4/book1.html.

Vimont, Daniel J. 2010. "Transient Growth of Thermodynamically Coupled Variations in the Tropics Under an Equatorially Symmetric Mean State ∗." *Journal of Climate* 23 (21): 5771–5789. doi:10.1175/2010JCLI3532.1.

Wong, Sun, Andrew E. Dessler, Natalie M. Mahowald, Peter R. Colarco, and Arlindo da Silva. 2008. "Long-term Variability in Saharan Dust Transport and Its Link to North Atlantic Sea Surface Temperature." *Geophysical Research Letters* 35 (7) (April 8): 1–5. doi:10.1029/2007GL032297. http://www.agu.org/pubs/crossref/2008/2007GL032297.shtml.